Bellcomm, Inc.

CENTRIFUGALLY OBTAINED ARTIFICIAL GRAVITY

April 4, 1969

D. B. Hoffman
R. E. McGaughy

Work performed for Manned Space Flight, National Aeronautics and Space Administration under Contract NASW-417.

TABLE OF CONTENTS

ABSTRACT

We investigated the effects of the centrifugal field in rotating space stations on the crew because centrifugally obtained artificial gravity is being considered for space stations. The astronauts will experience an unusual environment which is caused by:

1. A much larger Coriolis force, relative to the nominal gravity strength, than on Earth.

2. The much larger head to toe gravity gradient present in a rotating space station.

3. The asymmetry of forces for motions of different velocities.

These factors influence particle kinematics as observed by the astronaut, and could interfere with normal task performance and every-day activities. The magnitude of these unusual effects increases when the height (h) above the floor at which the activity occurs increases relative to the radius of rotation (R). Our work indicates that if h/R exceeds approximately 0.1, the effects become large enough to seriously hamper performance of ordinary tasks in the space station. (Other investigators have recommended that ω be 6 rpm or less for physiological reasons.) Finally, a counter-rotating inertial hub will be required for docking and crew transfer. A hub of large radius is necessary to provide a habitable environment for the crew while the hub is gradually spun up in order to acclimatize the crew to the rotating field. This process could take several days. The need for a hub eliminates consideration of tethered rotation configurations.

CENTRIFUGALLY OBTAINED ARTIFICIAL GRAVITY

I. INTRODUCTION

In-flight artificial gravity obtained by spacecraft rotation has often been suggested to improve astronaut physical fitness and habitability for long duration space flights (Refs. 1-6).

The primary physiological effect of rotation is canal sickness, which results from over-stimulation of the vestibular apparatus. The effects of rotation on vestibular function have been considered exhaustively elsewhere, and some of these results are available in References 4 and 5. These studies show the constraints on space station design imposed by human response to rotation. Based on this information, recommendations that the artificial gravity level be at least 0.3 g and the rotation rate not exceed 6 rpm for physiological acceptability have been made (Ref. 6). A number of disadvantages of rotationally induced artificial gravity are discussed in Ref. 6. Inclusion of artificial gravity is expected to influence spacecraft design (Refs. 1-6).

In this report the physical nature of the "gravitational" field obtained by spacecraft rotation is discussed and the kinematics of freely-falling objects as viewed by an astronaut are described. These kinematics are expected to be different from those in a real gravity field, but have not been described by other authors. Some consequences of the artificial field for astronaut performance and spacecraft design and habitability are discussed.

II. CHARACTERISTICS OF THE ROTATING ENVIRONMENT

A. Quantitative Differences Between the Earth's and Rotational Gravity Environments

Artificial gravitational fields obtained centrifugally (e.g., with rotating spacecraft or tethered rotation) differ in two important ways from the "true" gravitational field which we experience on Earth:

1. The effects of rotation are much larger in the spacecraft than on Earth, because the Coriolis acceleration* is much larger relative to the radial acceleration in the spacecraft. For example, a man walking at 5 ft/sec (3.4 miles per hour) on Earth experiences a Coriolis acceleration of only 2.3×10^{-5} times the vertical pull of gravity. But if he walks with the same speed along the floor of a 50 foot radius space station which rotates at 6 rpm (a "gravity" strength of 0.617 g), the Coriolis acceleration is one-third as large as the centrifugal field strength. Therefore, rotation effects on man in such centrifugal fields cannot be ignored.

2. Centrifugal fields produced by rotating space stations are more non-uniform than the Earth's gravitational field. On the Earth the fractional change in the gravity field over a distance of 5 feet (the gravity gradient) is 4.7×10^{-6}, whereas in the 50 foot radius space station it is 0.1.

The implications of these effects for man and manned space operations will be discussed in Section III.

B. Physical Nature of Centrifugal Fields

The force between objects in a gravitational field is a central force related to the mass of the objects and their distance of separation. This attractive force requires no transport medium between the objects. The centrifugal field, however, is essentially a constraint force. In order for a particle to be at rest in a rotating frame, it must be constrained to follow what is really a circular path about the axis of rotation.

If an object follows any circular path of radius R with a constant angular velocity ω', the acceleration experienced by it is directed radially with a magnitude $|\vec{a}| = (\omega')^2 R$. If this object is traveling with a velocity v along the inside of a circular track, then $\omega' = v/R$ so the acceleration is $(v/R)^2 R = v^2/R$. But if the circular track itself rotates with velocity ω, then $\omega' = \omega \pm v/R$ (the plus sign corresponding to v being in the same direction as ωR) and the acceleration is:

---

* The Coriolis acceleration has a magnitude $2\omega v \sin\gamma$ where ω is the angular velocity of rotation (radians/sec), v is the velocity of the object relative to the rotating frame, and γ is the angle which the direction of motion makes with the axis of rotation.

$$|\vec{a}| = (\omega \pm v/R)^2 R = \omega^2 R \pm 2v\omega + v^2/R. \qquad (1)$$

This is the acceleration experienced by an object moving along the "floor" of a rotating system in the absence of gravitational forces. The force experienced by the object is F = ma, and since it depends upon the velocity of travel, the force field is not conservative. (This can be demonstrated by showing that curl F $\neq$ 0.) This means that potential energy is not a unique function of position in such a rotating system because the work done in going from one point to another depends upon how fast the object travels and the path along which it moves as well as the distance between the points. It is impossible to say uniquely that one point in the spacecraft has a potential energy higher than another point.

C. Kinematics of Freely-Falling Objects Observed from a Rotating Reference Frame

An observer fixed in a rotating system sees objects move differently than he expects from his training and experience on Earth. This could lead to habitability, safety, and task performance problems on a rotating spacecraft. In this section we describe the trajectories of objects under free fall conditions (no externally applied forces) as seen by such an observer fixed in a rotating frame (e.g., a space station).

We used a rotating cylinder of radius R as shown in Figure 1 as our model of a rotating space station. The rotational motion is counter clockwise about the axis of symmetry perpendicular to the figure. The floor of this "spacecraft" is at a distance R from the center. The results of the analysis of this geometry are general and applicable to other rotating systems with fixed radius of rotation (R) and angular velocity (ω).

The object is released at a height h above the floor with an initial velocity v_o at an angle α, measured from the direction of rotation (see Figure 1). Any components of motion in the plane perpendicular to the axis of rotation will exhibit the effects of rotation which we describe below. Components of motion parallel to $\vec{\omega}$ will behave as if they were in an ordinary gravitational field with a strength of $g(h) = \omega^2(R-h)$.

The trajectory equations as seen by an observer at the rim of the rotating system are:

$$(A\text{-}5) \qquad x' = (R-h)(\omega t \cos \omega t - \sin \omega t) + v_o t \cos(\omega t - \alpha)$$

$$(A\text{-}6) \qquad y' = R-(R-h)(\omega t \sin \omega t + \cos \omega t) - v_o t \sin(\omega t - \alpha)$$

where R, h, and ω are defined above, v_o is the initial velocity of the object and α is the initial angle of travel. These equations are derived in Appendix A.*

In order to illustrate what these equations imply, we will discuss the effect of varying the parameters v_o, α, and h on the trajectory of an object in free fall in the spacecraft. The following descriptions apply only to the components of motion in the plane of Figure 1.

1. Zero Initial Velocity

If the object is released from a height h above the floor, the trajectory followed is independent of the magnitude of ω and R, and depends only on the ratio h/R (Appendix A, equations A-5, A-6 and B-20). Representative free fall trajectories for several values of h/R (with v_o=0) are plotted in Figure 2. It can be seen that the objects drift behind the observer as they fall (assuming the observer faces the direction of rotation, or toward α = 0). The object will land on the floor an angular distance ψ behind the observer.

This drifting behavior can best be understood by viewing the rotating system from an inertial (non-rotating) reference frame centered at the axis of rotation. From this vantage point, the floor is traveling in an arc at a constant speed ωR, whereas the object travels in a straight line at a smaller velocity ω(R-h) until it intercepts the floor of the spacecraft. Since ω(R-h) is smaller than the floor velocity, the point on the floor which was below the object when it was released would apparently always precede it. This intuition is verified by eq. B-21 which shows that ψ is always positive when v_o = 0.

If the object is dropped from increasing heights h, the velocity ω(R-h) imposed by the spacecraft's rotation decreases towards zero as h approaches R. Therefore, it takes an increasingly longer time for the object to reach the floor from larger h. During this time the floor is still moving in a circular arc at the velocity ωR, so that an observer on the floor sees complicated trajectories. For example, for h/R = 0.9 (Figure 2), the object appears to drift behind an observer facing the direction α=0, then rise, move forward, come back, and finally drift behind and upward again before reaching the floor. (For illustrative purposes we assume the spacecraft has no radial walls that would stop the particle, but only a

---

*We are indebted to T. Caruthers for writing a general computer program for finding the particle trajectory and velocity in terms of arbitrary initial conditions and rotating system parameters.

floor.) If the object were dropped from the center of rotation (h=R), it would not move at all with respect to either the inertial or rotating frame and it would never reach the floor.

As h approaches R, the angular distance traversed by the object before it lands (the angle ψ in Figure 2) progressively increases, as shown in Figure 3. When $\psi = 2\pi$, it lands at the observer's feet. Thus, in this simple cylindrical system, the observer could be exposed several times to the same falling object. In addition, except for very small h/R, the falling object initially appears to move laterally behind the observer rather than down as on Earth.

The quantity ψ depends only on h/R when $v_o = 0$. The time of flight, T (equation B-19), however, depends on ω as well as h/R. As h/R approaches 1.0, both ψ and T approach infinity.

2. Non-Zero Initial Velocity

The particle trajectories are different for objects released with an initial velocity v_o at different angles α. We will discuss the effect of v_o and h and several representative angles of departure separately. Equations A5 and A6 show that the trajectories are no longer independent of ω and R, as was the case for zero initial velocities.*

When the initial velocity is in the direction of spacecraft rotation ($\alpha = 0$), the object starts out horizontally as it would on Earth but falls faster. For small heights (h) it lands closer to the starting point than it would on Earth. This is shown for a particle with initial velocity of 5 ft/sec in a uniform gravitational field of 0.617 g for comparison (Figure 4). If it is released at increasing heights with the same velocity (as shown in Figure 5), it is in free fall long enough to acquire a noticeable backward drift. The resulting trajectories are similar to the case for $v_o = 0$ but the object

---

* We have somewhat arbitrarily chosen R = 50 feet and ω = 6 rpm as an example to define our rotating system. This combination results in a gravity strength of 0.617 times earth gravity at the floor. The rotation rate of 6 rpm is the maximum spin rate which man can tolerate without experiencing dizziness in performing "typical" operational tasks. R was chosen to be 50 feet because the relative gravity change occurring over the height of the man would be within currently accepted limits (15%) and a 50 foot radius could be reasonably obtained (Refs. 1-3).

always lands "closer" to the starting point (i.e., traversing a smaller angle, ψ, in Figure 5). For every height h there is always some velocity v_o which will cause the object to land at the observer's feet. This velocity is plotted in Figure 6 for α=0 in the rotational system we have chosen (R = 50 feet and ω = 6 rpm). It was found by evaluating ωT and β in equations B-15 to B-17 as functions of velocity and determining the v_o at which ψ = 0 in equation B-4.

Objects fixed in the spacecraft at height h above the floor move with velocities $\omega(R-h)$ (Figure 7). When an object is thrown vertically upwards from h_1 to h_2, it always acquires an initial forward velocity because the forward component of its velocity remains $\omega(R-h_1)$ but the local velocity of particles fixed in the spacecraft at height h_2 is $\omega(R-h_2)$, which is less than $\omega(R-h_1)$. For this reason the thrown objects appear to move forward, initially. The velocity equations, A7 and A8, are consistent with this idea because they show that when α = 90°, U_x is always positive at short times. Then, after the object has been in free fall for a sufficient time, it again acquires a backward velocity component, as was the case for zero initial velocity.

Figure 8 shows how the trajectories are affected by a change in the magnitude of v_o. For velocities small compared with $\omega(R-h)$, it can be seen that the trajectory deviates slightly from that shown in Figure 2 where v_o = 0. For larger initial velocities the trajectories deviate increasingly from those for simply dropped particles (compare with Figure 2).

The effect of the initial height on the trajectories of objects thrown upwards (α = 90°) with fixed v_o is shown in Figure 9. At larger initial h both the beginning vertical and horizontal displacements increase. This is caused by the lower effective gravity at higher h which results in larger initial vertical displacement. Because the incremental vertical displacement is increased, the velocity difference $[\omega(R-h_1) - \omega(R-h_2)]$ is also increased, resulting in the observed increased horizontal displacement at larger h.

When the velocity is directed in the backward direction (α = 180°) opposing the motion of the spacecraft, it is possible to put a particle into orbit inside the spacecraft. At $v_o = \omega(R-h)$, the object is stationary in the inertial frame and, since the spacecraft floor is rotating in an arc with velocity ωR, the particle appears to travel parallel to the floor at the same height h and velocity v_o, at which it was released. The object, although it is in "free fall," never reaches the floor. Under these conditions equations A5 and A6 describe a circle concentric with the axis of rotation. If v_o is slightly more or less than $\omega(R-h)$, the object eventually lands.

Until now, we have described the trajectories for various fixed initial angles α when h and v_o vary. We now consider their characteristics as a function of α for fixed v_o and h. Some sample trajectories for various angles are shown in Figure 10 for v_o = 5 ft/sec and h = 5 feet. These trajectories show the characteristic backward drift which we have seen many times. In addition, the trajectories and therefore the time of flight are longer for the backward direction than for the forward. In a uniform gravitational field, however, the time of flight for any fixed v_o is the same for objects thrown at equal angles about the vertical.

The parameters v_o and α affect the time of flight T of a particle in motion within the spacecraft. The dependence of T (equation B-15) on these parameters is shown in Figure 11. Outside the range of angles α of approximately 50° to 200°, which we shall designate the "inversion range," the time of flight T uniformly decreases as v_o increases. On Earth the inversion range is from α = 0 to 180°. Outside this range (α between 180° and 360°, downwards) the object reaches the ground sooner if it is thrown harder.

At angles within the "inversion range," T increases as v_o increases from zero to ω(R-h). When v_o exceeds ω(R-h), T decreases again. In contrast, increasing v_o for objects thrown at angles lying within the inversion range on Earth (0° to 180°) continuously increases T.

In Figure 11, ω(R-h) is 28.1 ft/sec (see also Figure 7), and the curves for v_o of 25 and 31 ft/sec were chosen to bracket this velocity. T is infinity at $v_o = \omega$(R-h) and α = 180°, and the object is in orbit inside the spacecraft. Notice that as v_o approaches ω(R-h), T gets very large and extremely sensitive to small changes in α. The same is true for the angular distance of travel ψ. Whenever such conditions exist, performance and learning problems are increased.

III. IMPLICATIONS FOR ROTATING SPACE STATIONS

In this section we examine the consequences of the rotating environment described above for men performing tasks in an orbital space station. We first describe typical tasks which must be performed, then discuss the long-term physiological consequences of living in a rotating environment and, finally, we briefly discuss the design of the rotating system and the conduct of spacecraft operations.

A. Astronaut Tasks

Astronaut tasks can be discussed in terms of their component motions. (We have chosen a radius of 50 ft and an angular frequency of rotation of 6 rpm for our description of the rotating system.)

1. Vertical Motions

The trajectories of freely-falling objects dropped from small heights are not expected to deviate sufficiently from the vertical to cause major re-learning of ordinary tasks, but the effects will nevertheless be noticeable. Figure 2 shows that objects dropped from a desk top height (i.e., about 30 inches) will fall approximately six inches behind their expected point of impact. Of course, similar effects will occur during urination, pouring liquids, etc.

An initial vertical velocity of about 5 ft/sec is normally attained when arising from a chair. Figure 12 shows the calculated trajectory of an object (e.g., an astronaut) which started vertically from the floor with this velocity. (Since the center of mass of a man is approximately 3 feet above his feet, the actual trajectory would be intermediate between that shown in Figure 12 (v_o = 5 ft/sec) and the trajectory shown in Figure 10 for $\alpha = 90°$ and v_o = 5 ft/sec.) The astronaut would lurch forward noticeably as he rises, and he must learn how to counteract this effect. Similar effects are expected whenever a man jumps. If he should jump vertically very strongly (e.g., v_o = 15 ft/sec; a high jumper can raise his center of gravity almost three feet), then he would land 5.5 feet in front of his starting point (see Figure 12 for v_o = 15 ft/sec). In addition to the horizontal displacement, the jumper will also rotate through the angle ψ during the jump. In the example of the high jumper above, ψ is 6.3°.

The effect of spacecraft rotation on manual tasks involving vertical motions can be illustrated by considering the question of hammering a nail. It can be shown (Appendix C) that if a hammer is driven vertically towards a nail, it will undergo a lateral displacement from the target. For example, a 5 lb. hammer driven one foot vertically down with a force of 10 lbs. would miss its target by 0.78 inches. This effect would certainly be noticeable as different from Earth experience, and is representative of the effects which would accompany many tasks performed in a rotating space station.

2. Horizontal Motions

A man walking at 5 ft/sec at a radius of 8 feet from the center in a direction opposite to the direction of rotation would be weightless and would float until he hit a wall or until some other part of the spacecraft hit him. If he walked at the same speed but at a radius of 50 feet, he would experience a 34% increase in weight from the zero-velocity weight when traveling in the direction of rotation and a 30% decrease in weight when walking in the other direction (equation 1). This factor is large enough to demand major re-learning of tasks involving horizontal motions approaching 5 feet/sec (3.4 miles per hour), which is not an unusually large speed. (For example, if an object were thrown horizontally at 5 feet/sec on Earth from a height of 3 feet, it would land 2.2 feet from the observer's feet.)

Work Required for Walking

In order to estimate the work of walking in the rotating environment, we must know how the gravity level affects the relationship between the work of walking and walking speed. This knowledge is necessary because the effective gravity level in the rotational system depends upon the speed of travel, as noted above (equation 1).

The studies of Cavagna and co-workers (Refs. 7-9) furnish a formulation of the mechanics of walking that is clear and allows prediction on a quantitative gravity scale of the work required for walking. Their view of walking mechanics is that most of the potential energy, P, gained by a man as he elevates his center of gravity vertically is used to perform the work of slowing the body's forward motion after the heel touches the floor and to perform the internal muscular work associated with moving the joints. Although this potential energy is directly proportional to the "gravity" level, the two latter forms of work, T, are independent of gravity and increase with walking velocity as shown in Figure 13 (adapted from Ref. 7). The body is not raised progressively more as the velocity of walking increases. Therefore, the energy required to overcome the resistance to forward motion eventually exceeds the available potential energy, and the mechanics of locomotion (i.e., the gait) must change if higher velocities are to be attained. We can find v_{max}, the velocity beyond which the required internal energy exceeds the available potential energy, from Figure 13, which shows the experimentally-determined velocity dependence of the potential and internal energies. At velocities

higher than v_{max}, the gait changes to running, which requires more energy. Since the potential energy curve is proportional to the g level, we can predict the v_{max} for different gravity levels. This is done by scaling the P curve in Figure 13 according to the gravity level, and finding the velocity (defined as v_{max}) above which T is larger than P for each g level. The result is shown in Figure 14, where the gravity scale is normalized to Earth's gravity at sea level. Superimposed on the same graph are the operating curves for several different spacecraft designs. Notice that with a design in which $\omega^2 R = 0.617$ g, any choice of radius from 10 feet to 1000 feet results in a maximum walking speed of only 1.6 to 1.8 miles/hr. as compared to 3.9 miles/hr. at 1.0 g. We can obtain higher walking speeds only by going to designs in which $\omega^2 R$ approaches 1.0 g. Therefore, if Cavagna's analysis is correct, a man can walk normally at 0.617 g at a rate of only a little over half his maximum Earth speed.

Although this formulation of the mechanics of walking is clear and amenable to quantitative prediction for the effects of gravity strength, it is not supported by measurements of metabolic rate made by Wortz and Prescott (Ref. 10) in lunar gravity simulation experiments. They measured the metabolic rate (in BTU/hr) during walking as a function of velocity when the subject was partially suspended to simulate g levels of 1/4 g, 1/6 g and 1/8 g, and found that there is no discontinuity in metabolic rate at any speed between 0 and 4 mph. Wortz and Prescott make no statements about the gait necessary to achieve the various speeds, but Cavagna's mechanics would predict a change in gait above 1.5 mi/hr which one expects by analogy with Earth results would be accompanied by an increase in metabolic rate. This discrepancy is currently unresolved, but Wortz and Prescott's lunar simulation experiments nevertheless indicate that somehow it is possible to achieve speeds approaching 4.0 miles/hr with metabolic rates that are not excessive. In fact, these data indicate that walking at reduced gravity is less costly than at 1 g. Figure 15 shows the metabolic rate measured by Wortz and Prescott for 1.0 g. The curve for 0.617 g was obtained by interpolating their data, and the curve for the spacecraft was calculated from the same data but using the operating curve in Figure 14 corresponding to R = 50 feet. The metabolic rate is less for the spacecraft than for 0.617 g because the effective gravity level is reduced when walking counter to the rotation direction. The curve would be very close to the 1.0 g curve when walking in the direction of rotation. Note that the magnitude of the effect is about ±10% of the nominal metabolic rate at 3 miles/hour.

The measurements by Hewes, et al., at Langley Research Center (Ref. 11), on an inclined plane lunar gravity simulator provide a thorough description of the motions performed by man in walking and running at 1.0 g and 1/6 g. Although their data cannot be interpreted on a quantitative g scale, it is clear that in reduced gravity the body will lean forward more, the step distance will be longer, and the step frequency will be less than at 1 g. We expect that in rotating systems walking counter to the direction of rotation would result in the reduced-gravity effects described by Hewes, et al., and walking along the direction of rotation would have the opposite effect.

B. Physiological Effects

It is expected that man living in a centrifugal field for extended periods would physiologically adapt to the environment in several ways. The main effects expected include vestibular acclimatization, altered body fluid distribution and changed bone structure. The latter two effects are expected to be more severe in zero g environments.

When the spacecraft is initially set into angular motion from zero-gravity conditions, symptoms of motion sickness will be experienced by the crew if the increment in angular speed is too large (Ref. 12). Motion sickness can be avoided with small increments in rotation rate, but if it does occur, most people could adapt to the situation within a day. As long as the rotation rate remains low enough (below 6 rpm), such "vestibular" problems are not likely to be persistent.

A prolonged exposure to a centrifugal field is expected to affect the human body in two primary ways: (1) it changes the distribution of fluids (primarily blood), and (2) it influences the shape and internal structure of bone tissue.

Any change in the strength of the gravity field is expected to alter both the cardiovascular and the musculoskeletal systems. The 14-day Gemini flight (Ref. 13) has revealed the extent to which space flight in zero-gravity has caused the loss of body water, the depletion of calcium from the bones, and reduced "orthostatic" tolerance.* However, these effects cannot be predicted for a 3-month flight at 0.6 g because we have no knowledge about the progressive changes in man's response to any level of gravity strength.

---

* The ability of the cardiovascular system to redistribute blood after it has pooled in the legs.

In addition to having a reduced gravity, a rotating space station has a linear gradient of gravity strength, varying from zero at the center of rotation to a maximum at the floor. There is no data to indicate what physiological effects this gradient would have.

The pooling of blood in the legs is expected to be diminished in a gravity gradient environment because the blood column above the floor "weighs" less than it would in a constant gravity environment. This effect is in the same direction as the transfer from 1 g to weightlessness. This important area deserves more investigation.

It is known that bone tissue calcifies along the internal lines of stress and grows locally in response to local mechanical stress (Ref. 14). Therefore, one might expect that after a man has adapted to a gravity gradient environment, his leg bones will be thicker and the bones of his upper extremity lighter than they would be without a gradient. The time required for this adaptation to be complete should be about the time it takes for broken bones to heal (perhaps two months). This phenomenon has not been considered in the design of reentry tasks and hardware for long duration flights.

C. Design Considerations

1. Free Falling Objects

The free-fall trajectories we have described above have shown that if objects (including astronauts) are thrown or dropped at large heights (h approaching R, the radius of rotation), they will follow highly unusual paths before they land on the floor. These objects could present hazards to astronauts particularly when h/R is large, if the object is sharp or heavy, or if the astronaut is in a pressure suit. Cross sectional walls could prevent particles from dropping in one section of the station and landing far away. Ceilings could act as umbrellas and also prevent danger from objects freed at large h/R.

2. Design Parameters

The human factors implications of artificial gravity for the design and operation of spacecraft have been considered by many authors including References 1, 2, 3, 6, 15, 16, 17 and 18. The Coriolis effect leading to weight changes and disturbances of vestibular function (orientation and canal sickness) has had the most impact on design guidelines of rotating systems.

Disturbances of the stability of rotation could cause significant nutation and precession of the space station. Such effects would stimulate canal sickness, etc., as well as impact unfavorably on astronomy and other scientific experiments. There is a dramatic increase in rotational stability for a larger radius rotating space station (Ref. 19). Increasing the radius from 30 to 150 feet decreases instabilities introduced by crew motions and docking impacts by factors exceeding 10. Newsom and Brady's studies (Ref. 15 and 18) showed, however, that performance was not appreciably affected by instabilities within expected ranges.

The results derived from all of the cited studies have yielded design parameters limiting the rotational rate and radius of rotation, and are shown in Figures 16 and 17. The maximum rotational rate is limited by the onset of canal sickness and is currently believed to be 6 rpm (Ref. 17). This result was obtained from consideration of the torque value on the endolymph resulting from nominal head rotation. A lower limit for artificial gravity has been determined to be about 0.3 g, below which locomotion ceases to be efficient (Ref. 2) The lower limit in radius is determined either by the arbitrary assignment of a 15% heart to foot gravity gradient relative to floor ambient gravity (Fig. 16 and Refs. 1-3), or by assuming that a reasonable upper bound to apparent change in body weight when walking is 20% (Fig. 17). In either case the lower limit on radius of rotation is about 40 to 50 feet for an assumed walking speed of 3 ft/sec. These guidelines are subject to change, especially if astronauts are selected for insensitivity to rotationally induced effects.

3. Activities

Docking and resupply activities will be difficult with both of the two currently-discussed methods of obtaining artificial gravity. In tethered rotation, docking and resupply will require termination of rotation or delicate maneuvering by the resupply ship because a hub cannot be employed. This is costly in fuel, difficult to achieve, and requires great astronaut skill. This is unfortunate, because by the time space stations with artificial gravity become feasible, astronauts should be selected primarily for scientific or medical skills rather than piloting ability.

If the centrifugal field is obtained by simple rotation of a dumbbell, cylinder, toroid, or derivative shapes about a principal axis, then maintenance and EVA activities will be difficult because of Coriolis and centrifugal effects.

In either case, EVA will require restraints at all times. Without them the astronaut would be flung from the space station. While constrained, he will be subjected to whatever rotational forces are present at that point. His tools must also be restrained. In addition, within the spacecraft, tools, nuts, bolts, etc., may be at least as difficult to control as in weightlessness, and loose objects would behave as discussed above.

A rotating space station will probably incorporate a counter-rotating hub at the center. For example see Fig. 20. This hub would rotate at the same speed as the space station in order to provide a zero-gravity platform for scientific experiments and to make it easier for an incoming vehicle to dock with the station. Equipment transfer from such a hub to the other parts of the station will be difficult, however, unless the hub is rotated in the same direction and at the same speed as the space station. When this happens, the transferring crew for a period of time will be in a rotating chamber with a very small radius, and most tasks will be performed at heights where h/R approaches 1.0. We have shown that unusual effects are expected close to the center of rotation. Under these conditions it is likely that the astronaut will be rotating about an axis through his body, a situation which is almost certain to produce motion sickness as well as total body disorientation. The best way to avoid these problems is to spend as little time close to the center of rotation as possible. This means that new packaging and automated handling techniques will be desirable for resupplying space stations.

Sudden exposure to rotating environments may cause canal sickness (Ref. 16). Thus new crews or those who must work on the zero g laboratory may have to be gradually acclimatized to rotation. Experiments indicate that 1.5 to 3.6 rpm increments are acceptable for this purpose (Ref. 12).

There are several implications of these experiments for our spacecraft situation. First, it would be desirable to "spin" the crew or hub up or down in steps to allow incremental adaptation. Second, crew exchange may be complicated in the rotating station for both new and old crews. It may be desirable to clutch the hub to permit gradual exposure of the new crew to increasing rotation rates and vice versa for the debarking crew. This procedure, similar to decompression of divers, could take several days. Our calculations indicate that the hub should be large to minimize h/R as much as possible during the extensive crew acclimatization period which may be necessary before crew transfer.

If the hub is used as a laboratory for zero g experiments or as an astronomy lab, then the experiments will be interrupted during crew acclimatization to the rotating environment. One possible solution to this problem is to design the spacecraft in a three concentric ring configuration. The center hub could be counter-rotating for docking and could be spun up to the speed of the rotating space station itself (the middle ring) for crew transfer. Zero gravity experiments could proceed uninterrupted if they were housed in a third outer counter rotating ring or a dynamically balanced set of counter-rotating section. "Elevators" on rails between the sections could be used to gradually acclimatize the man to the environment to which he is transferring. Detailed consideration should be given to such design problems and to the problem of crew and equipment transfer between differentially spinning sections.

IV. SUMMARY AND CONCLUSIONS

Centrifugally obtained artificial gravity and normal Earth gravity differ physically. The primary differences experienced by the astronauts arise from the much larger Coriolis force and gravity gradients relative to the nominal gravity environment in the space station. Additionally, the rotationally obtained field is inhomogeneous since effects depend on the direction of the astronaut's activity.

These factors affect the particle kinematics as seen by an observer (astronaut) in the rotating station. In general, the trajectories differ from those expected from his Earth experience and he must adapt to the new environment. For example, dropped objects will drift counter to the direction of rotation as they fall and will land an angular distance ψ on the floor away from the observer. Rigid bodies will rotate through the angle ψ during flight. The effects are increasingly unusual as h/R, the particle height to radius ratio, approaches 1.0. Thus, it is desirable to design spacecraft so that normal working activities take place at small heights (h) relative to the radius (R) (i.e., minimize h/R within engineering constraints).

Astronauts will experience forces and torques while performing such simple tasks as rising, walking, hammering, pouring water, etc. For example, upon rising from a chair the astronaut will lurch towards the direction of rotation. In addition, in a space station in which R = 50 ft and ω = 6 rpm, an astronaut hammering a nail on the floor would miss the target by over 3/4 inches.

Increases and decreases in weight while walking along the floor are expected, and these will affect the work of walking. In addition, the maximum speed of normal walking is limited for motion in the counter rotation direction. In our case (R = 50 ft, ω = 6 rpm) his maximum walking speed in the counter direction is expected to be only about half the normal walking speed on Earth. Each of these phenomena is a small but noticeable effect when taken singly, and the astronaut should be able to eventually learn how to manipulate objects as well as control his own weight if he is not pressed for time and if he restricts his activities to regions in which h/R does not greatly exceed 0.1. At larger h/R (i.e., when h/R approaches 1.0) tasks become increasingly difficult to perform. These effects could seriously hamper manned operations near the hub of a rotating space station.

The primary physiological problem expected in rotating space stations is canal sickness. This problem has been intensively investigated by others who showed that canal sickness can be avoided by keeping the rotational rate below 6 rpm. However, more subtle long range physiological effects such as redistribution of body fluids and bone calcium may occur. For example, there will be less pooling of blood in the astronaut's legs because of the large head to foot gravity gradient in a rotating system. Therefore, from this standpoint, artificial gravity is not as effective in counteracting weightlessness as the nominal "gravity" strength $\omega^2 R$ would indicate. In addition, we expect that within about two months the leg bones would thicken while bones in the upper extremities would become more fragile as a response to the altered distribution of mechanical stress in a gravity gradient.

Activities such as docking, resupply, and crew transfer will require a hub which rotates counter to the space station at a speed which maintains a zero-gravity platform. The hub could also serve as an inertial platform for astronomy and Earth sensing experiments. New crew members may require gradual acclimatization to the rotating environment accomplished by an incremental spin up process which may take several days to complete. Thus the hub should have as large a radius as possible, since it must be habitable during the acclimatization periods and allow acceptable task performance during resupply.

Of the two generally mentioned configurations, spacecraft rotation about a principal axis and tethered rotation, the first is preferred because it allows docking, resupply, and crew transfer without stopping space station rotation.

D. B. Hoffman

R. E. McGaughy

1011-$\frac{DBH}{REM}$-cb

Attachments
References
Figures 1 - 20
Appendices A - C

REFERENCES

1. Dole, S. H. "Design Criteria for Rotating Space Vehicles." Research Memo 2668. Santa Monica, Rand Corporation, 1960.

2. Loret, B. J. "Optimization of Space Vehicle with Respect to Artificial Gravity." Aerospace Medicine 34: 430. 1963.

3. Payne, F. A. "Work and Living Space Requirements for Manned Space Stations. In "Proceedings of the Manned Space Stations Symposium." New York, Institute of Aeronautical Sciences, 1960.

4. "The Role of the Vestibular Organs in the Exploration of Space." NASA-SP-77. Washington, D. C., 1965.

5. "Third Symposium on the Role of the Vestibular Organs in Space Exploration." NASA-SP-152. Washington, D. C., 1967.

6. Kontaratos, A. N. "On the Question of Artificial Gravity." Memorandum For File. Washington, D. C., Bellcomm, Inc., August 23, 1968.

7. Cavagna, G. A., and R. Margaria. "Mechanics of Walking." J. Appl. Physiol. 21(I): 271. 1966.

8. Cavagna, G. A., et al. "Mechanical Work in Running." J. Appl. Physiol. 19(2): 249. 1964.

9. Cavagna, G. A. "Human Locomotion at Reduced Gravity." J. British Interplanetary Society 21: 166. 1968.

10. Wortz, E. C., and E. J. Prescott. "Effects of Subgravity Traction Simulation on the Energy Costs of Walking." Aerospace Med. 37: 1217. 1966.

11. Hewes, D. E., et al. "Comparative Measurements of Man's Walking and Running Gaits in Earth and Simulated Lunar Gravity." NASA TN D-3363. Washington, D. C., 1966.

12. Bergstedt, M. "Stepwise Adaptation to a Velocity of 10 rpm in the Pensacola Slow Rotation Room." In "The Role of the Vestibular Organs in the Exploration of Space." NASA SP-77. Washington, D. C., 1965.

13. "A Review of Medical Results of Gemini 7 and Related Flights." Held at Management Center, John F. Kennedy Space Center, Kennedy Space Center, Florida, 1966.

14. Lockhart, R. D., et al. "Anatomy of the Human Body." Philadelphia, J. P. Lippincott, 1959.

15. Newsom, B. D., and J. F. Brady. "Observation on Subjects Exposed to Prolonged Rotation in a Space Station Simulator." In "The Role of the Vestibular Organs in the Exploration of Space." NASA SP-77. Washington, D. C., 1965.

16. Graybiel, A., et al. "The Effects of Exposure to a Rotating Environment (10 rpm) on Four Aviators for a Period of 12 Days." In "The Role of the Vestibular Organs in the Exploration of Space." NASA SP-77. Washington, D. C., 1965.

17. Thompson, A. B. "Physiological Design Criteria for Artificial Gravity Environments in Manned Space Systems." In "The Role of the Vestibular Organs in the Exploration of Space." NASA SP-77. Washington, D. C., 1965.

18. Brady, J. F., and B. D. Newsom. "Revolving Space Vehicle Stability Requirements for Perceptual-Motor Tasks." International Astronautical Federation Paper B118. 1968.

19. Kurzhals, P. R., et al. "Space Station Dynamics and Control. A Report on the Research and Technological Problems of Manned Rotating Spacecraft." NASA TND-1504. 1962.

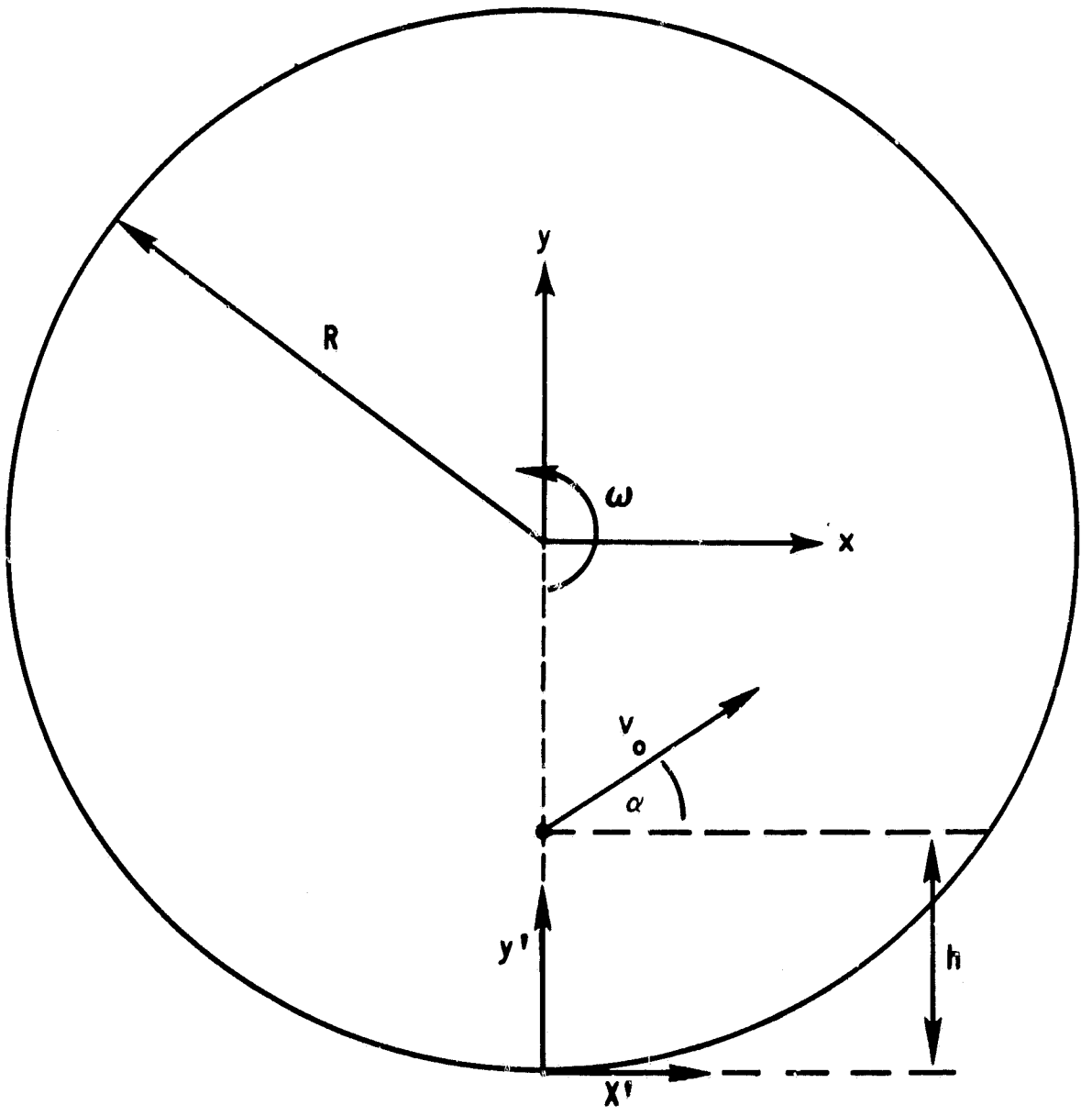

FIGURE 1 - ROTATING SYSTEM GEOMETRY

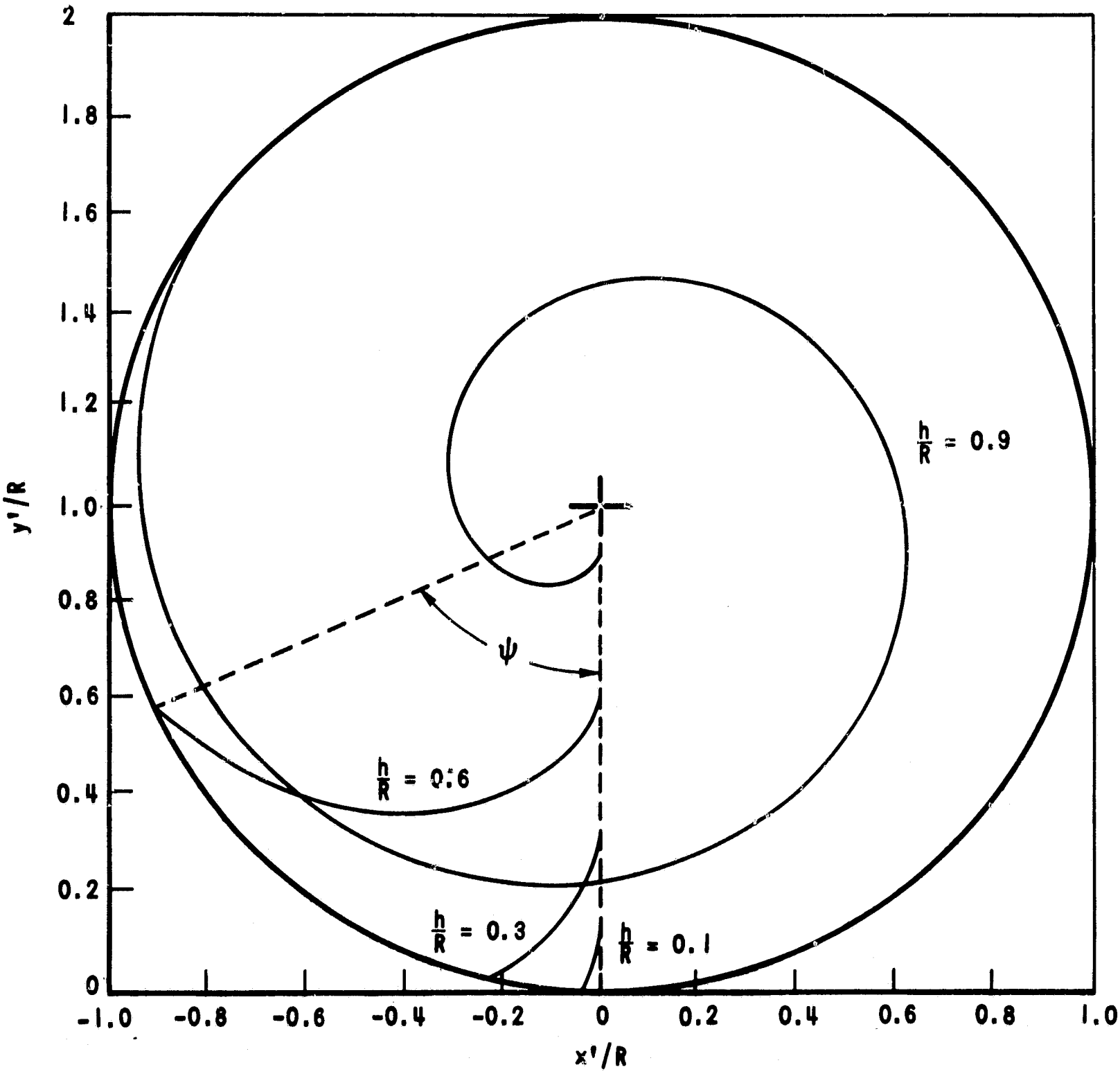

FIGURE 2 - FREE-FALL TRAJECTORIES OF DROPPED OBJECTS FOR $v_o = 0$

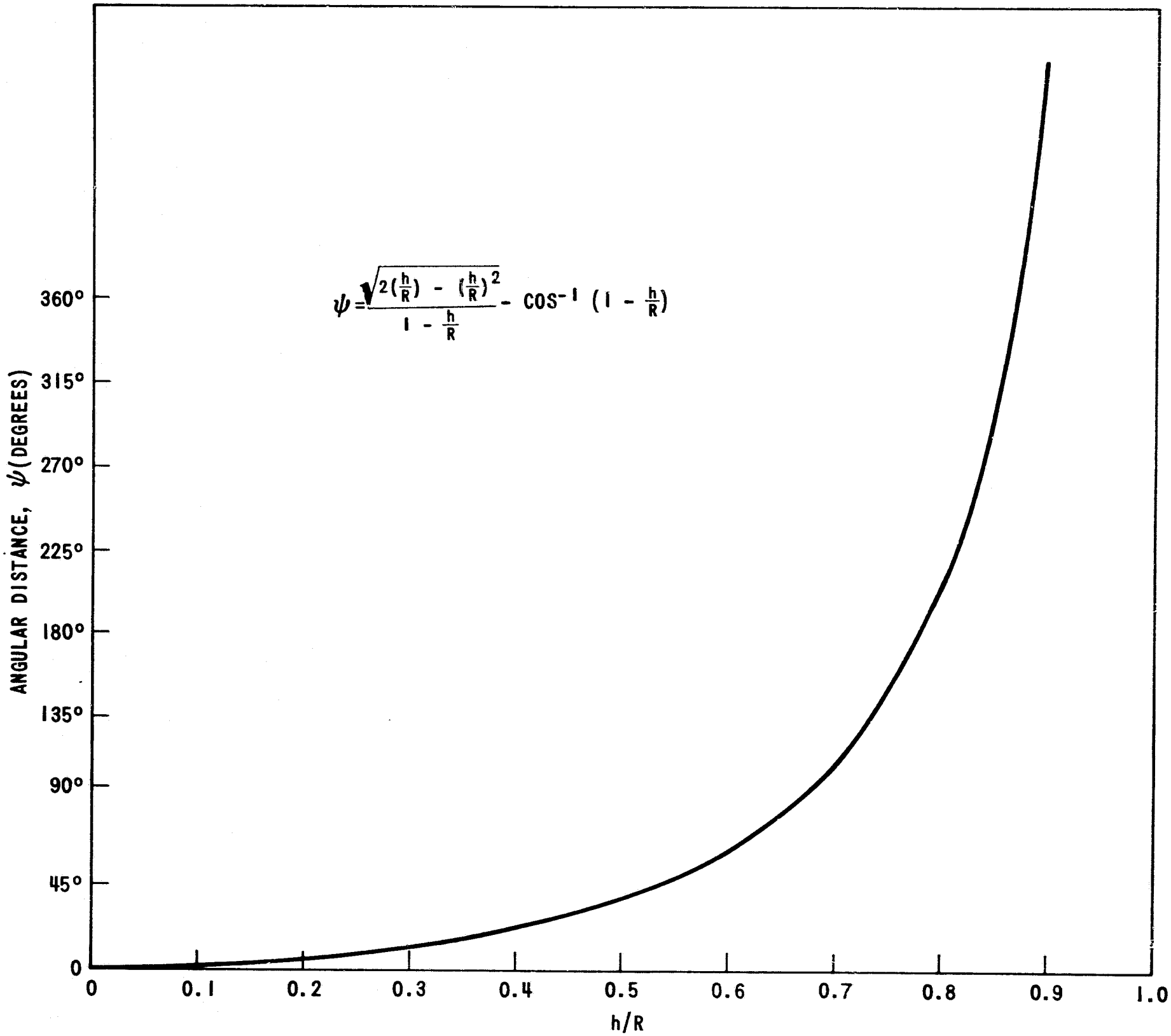

FIGURE 3 - ANGULAR DISTANCE OF TRAVEL
FOR DROPPED OBJECTS

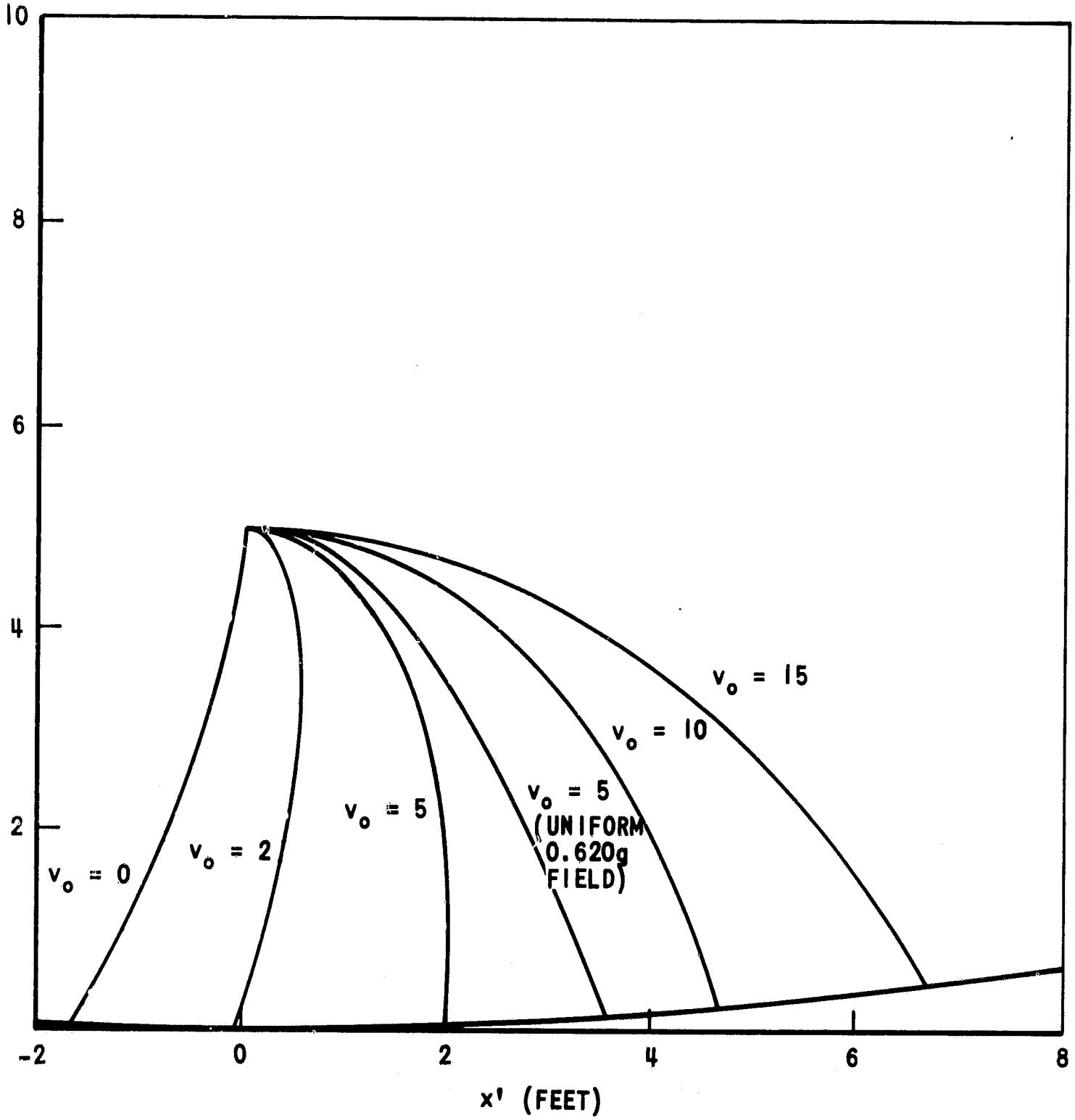

FIGURE 4 - THE EFFECT OF v_o ON PARTICLE TRAJECTORIES FOR $\alpha = 0$, $h = 5$ FEET

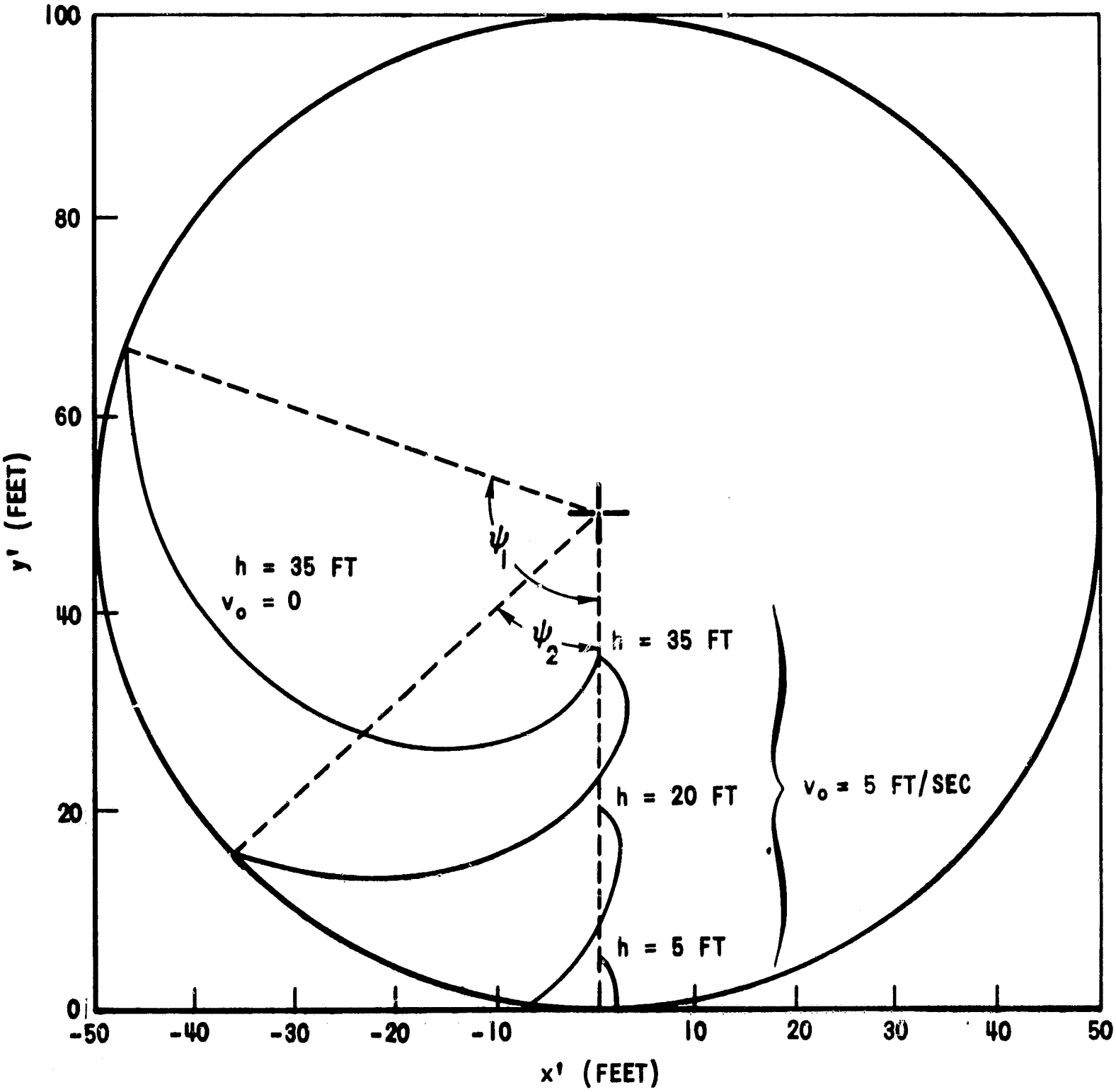

FIGURE 5 - THE EFFECT OF h ON PARTICLE TRAJECTORIES, FOR $\alpha = 0$, v_o = 0, 5 FEET/SEC

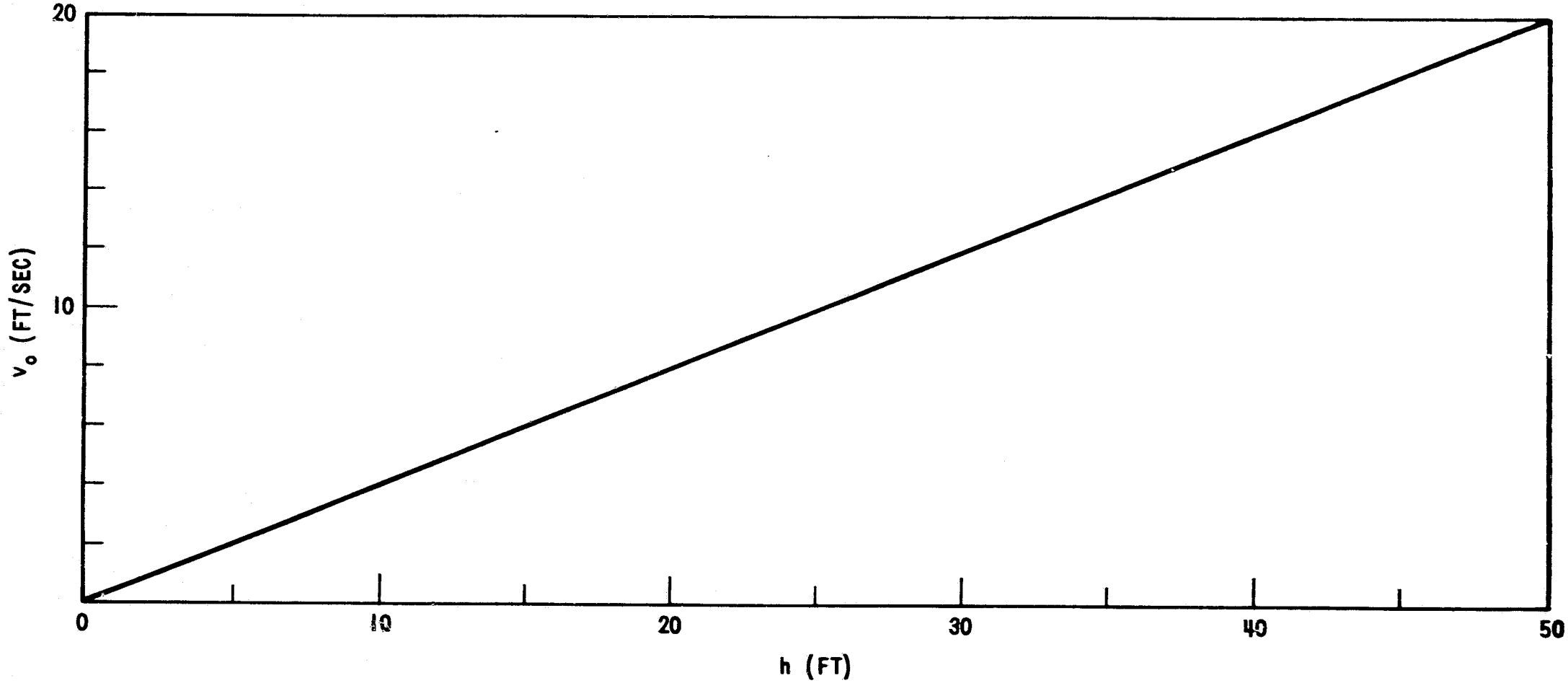

FIGURE 6 - THE INITIAL HORIZONTAL VELOCITY AT $\alpha = 0$, REQUIRED FOR THE OBJECT TO LAND AT THE THROWER'S FEET ($\psi = 0$) WHEN RELEASED FROM VARIOUS HEIGHTS h

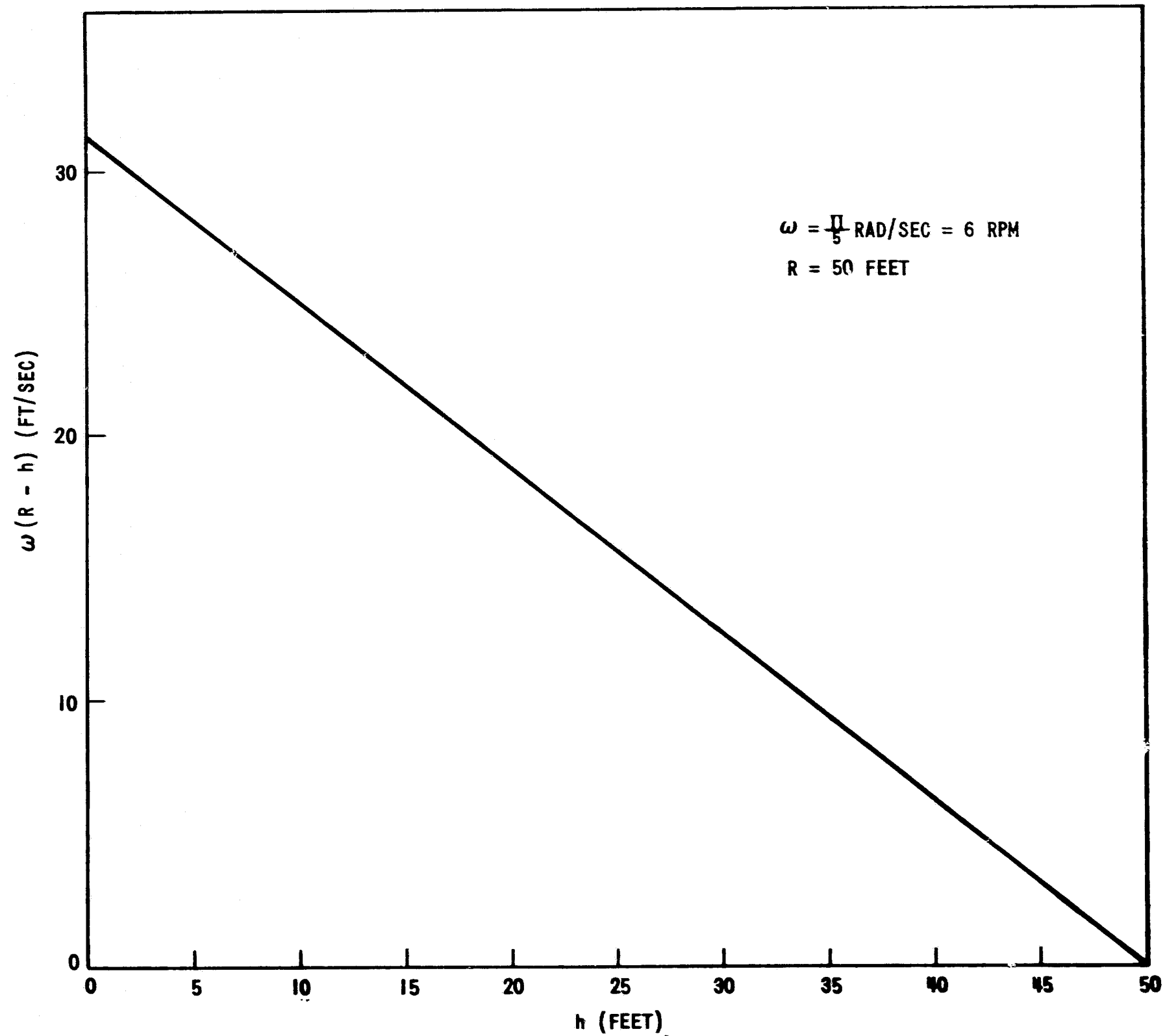

FIGURE 7 - INERTIAL VELOCITIES OF THE ROTATING SYSTEM
vs. HEIGHT ABOVE FLOOR

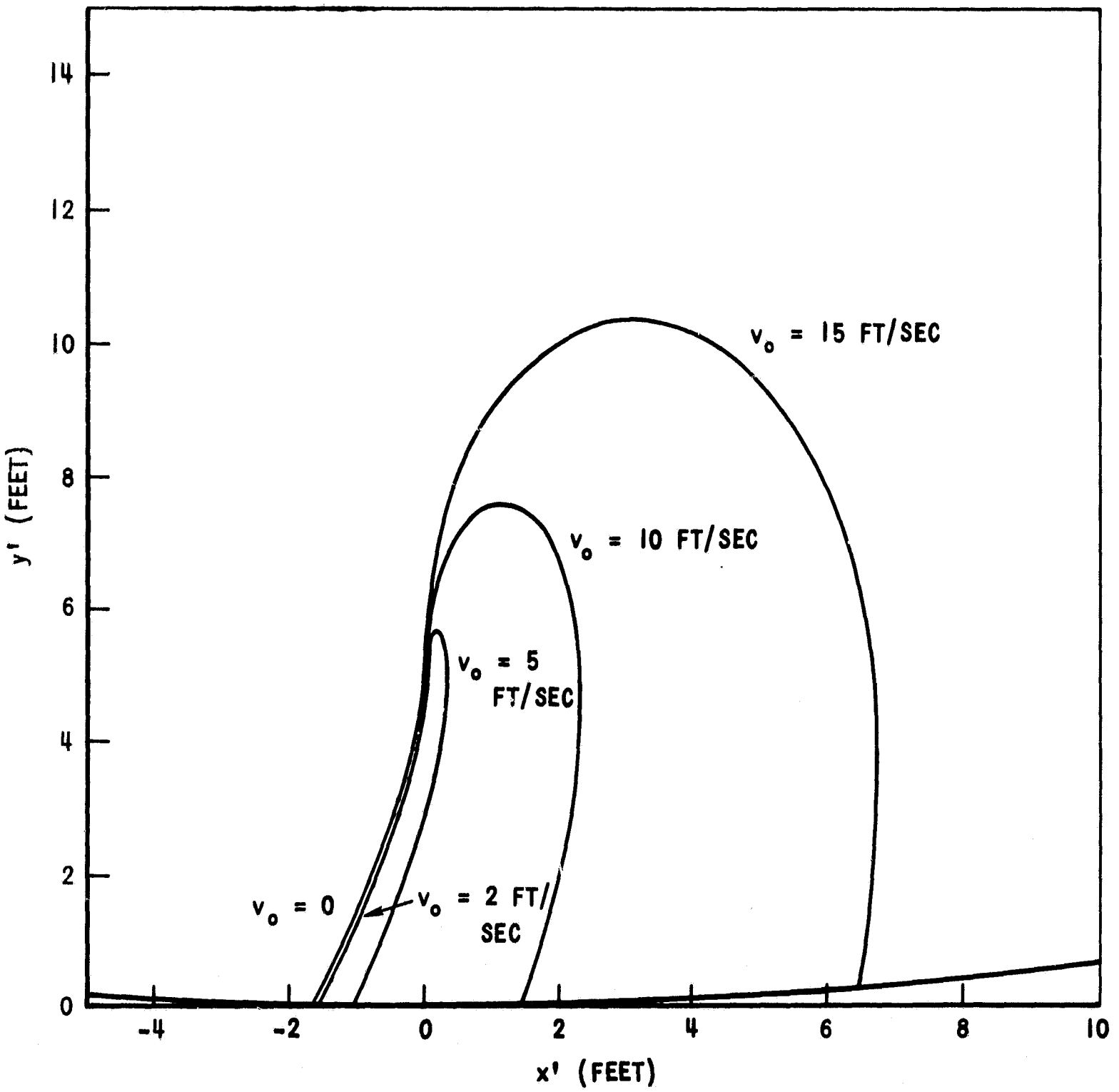

FIGURE 8 - THE EFFECT OF v_o ON PARTICLE TRAJECTORIES FOR $\alpha = 90°$, h = 5 FEET

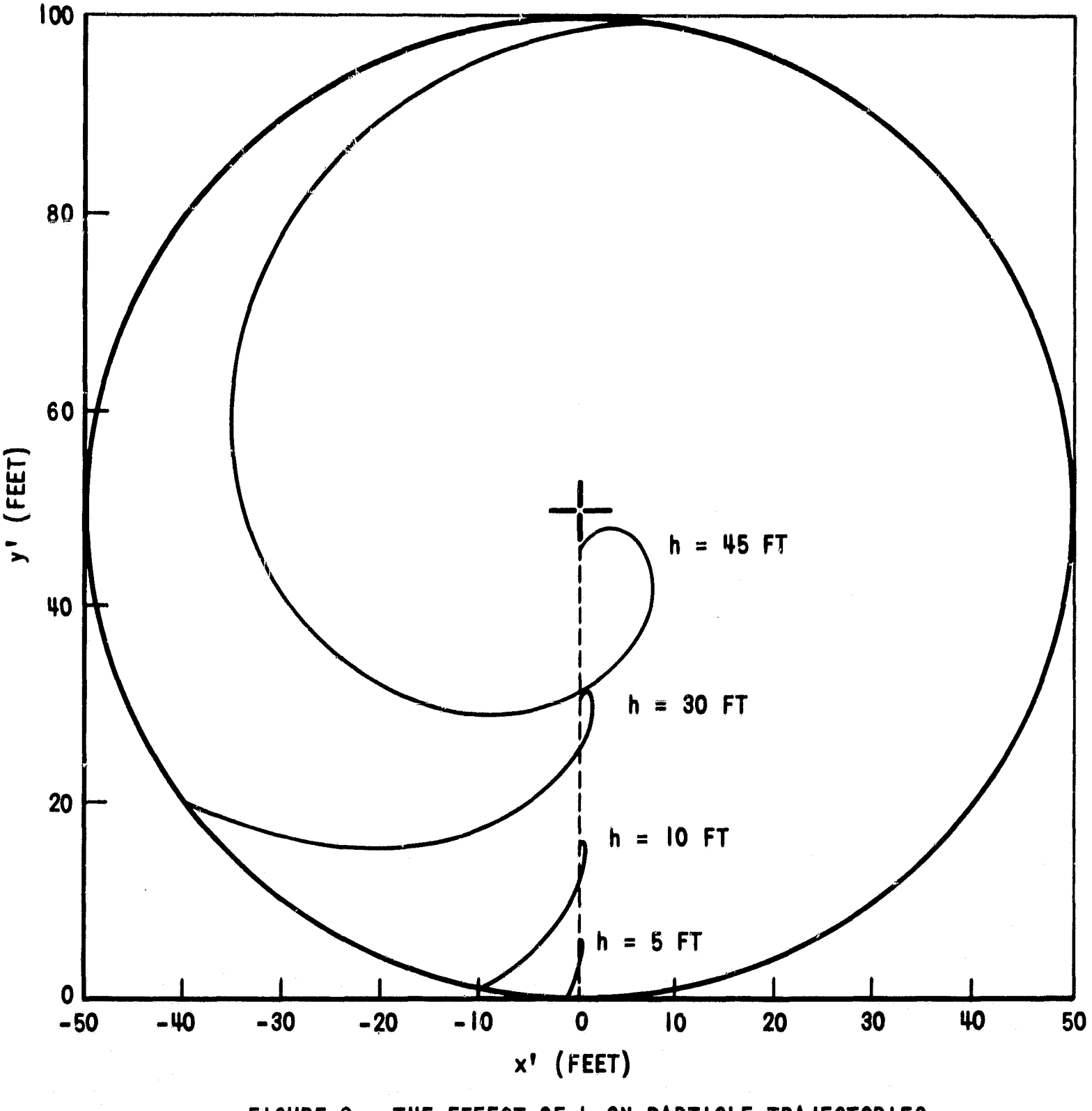

FIGURE 9 - THE EFFECT OF h ON PARTICLE TRAJECTORIES FOR $\alpha = 90°$; $v_o = 5$ FT/SEC

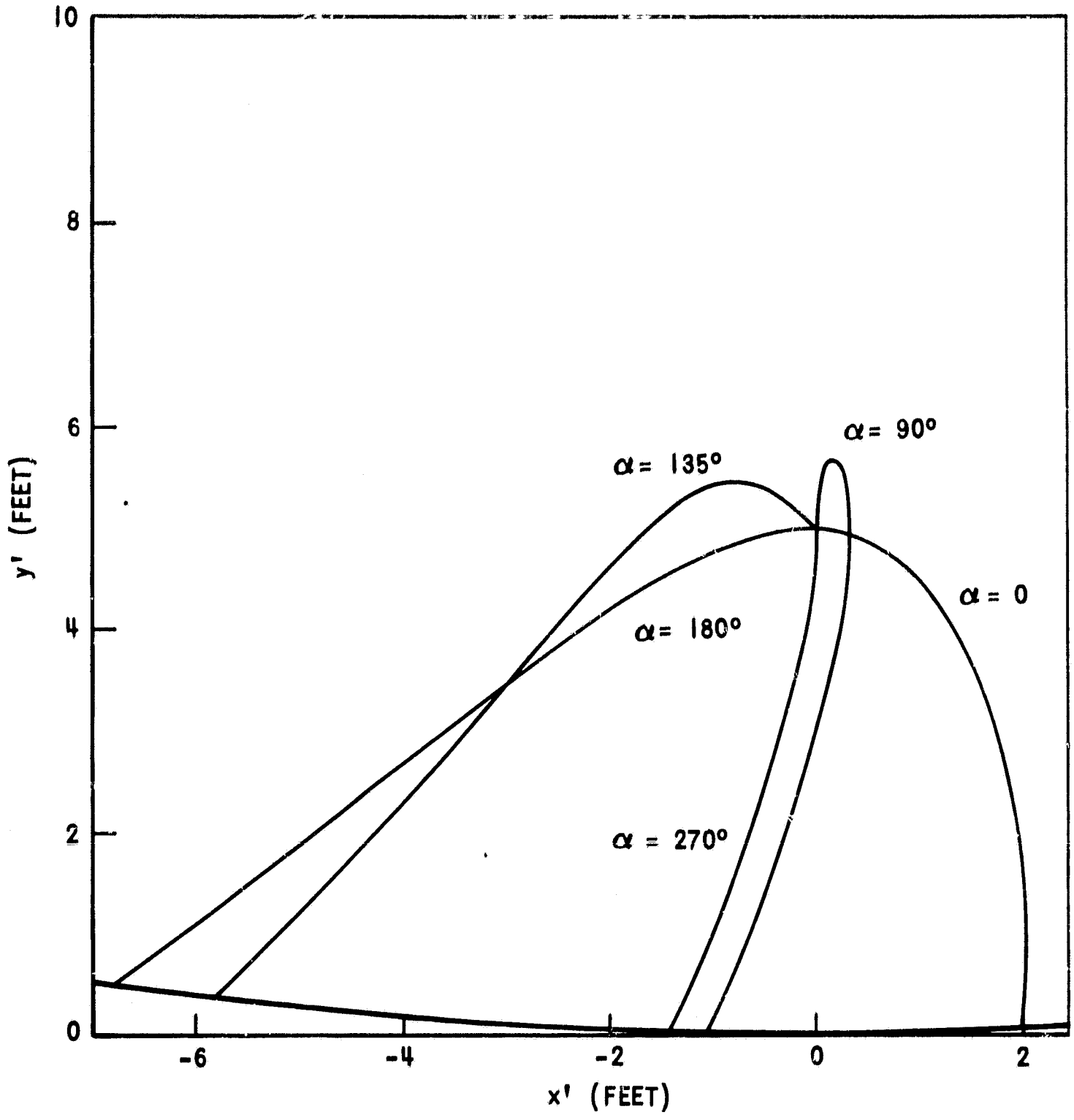

FIGURE 10 - THE EFFECT OF α ON THE PARTICLE TRAJECTORIES FOR v_o = 5 FT/SEC, h = 5 FEET

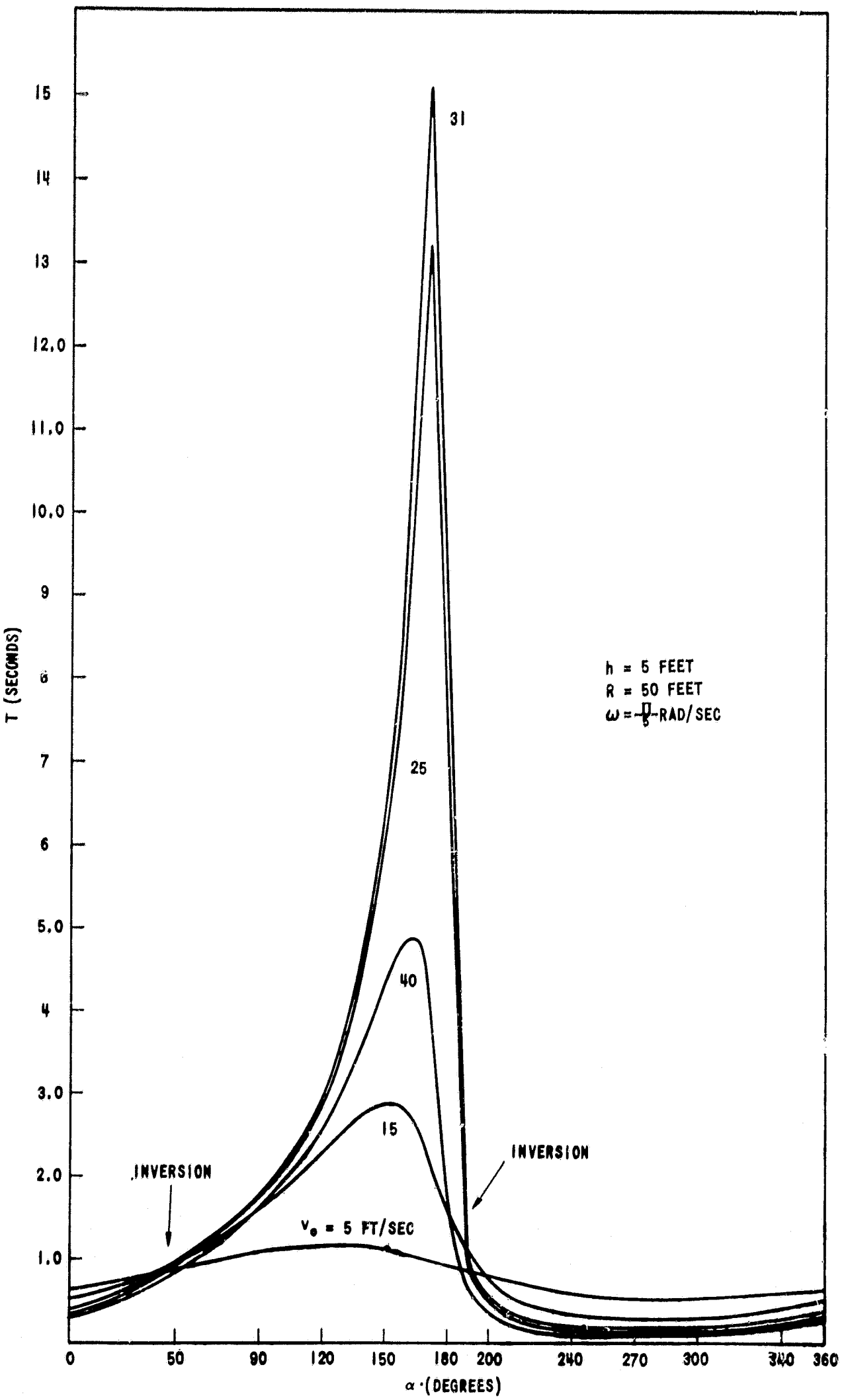

FIGURE 11 - EFFECT OF α AND v_0 ON TIME OF FLIGHT

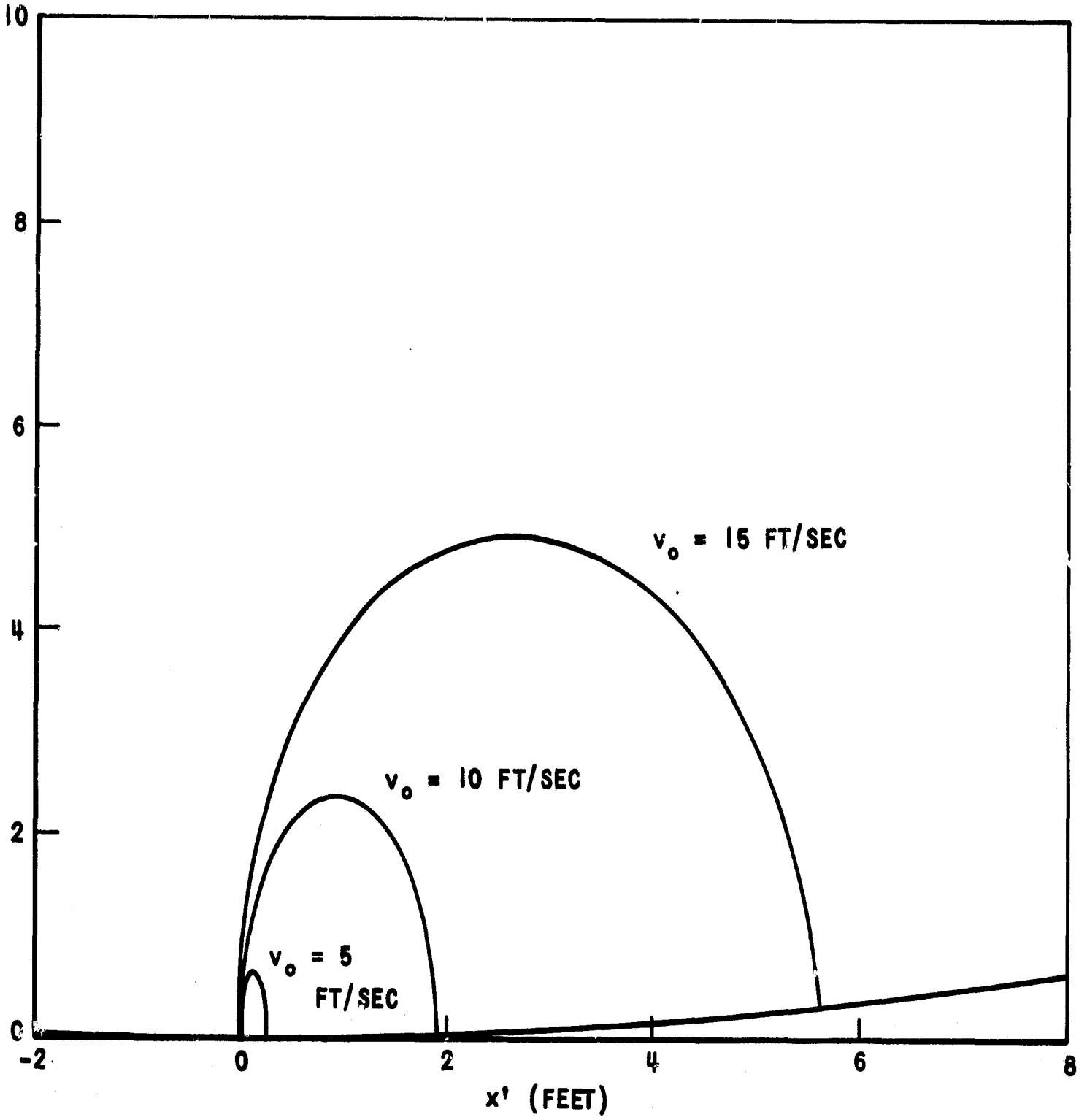

FIGURE 12 - TRAJECTORIES FOR OBJECTS RELEASED FROM FLOOR AT VARIOUS VELOCITIES, h = 0, α = 90°

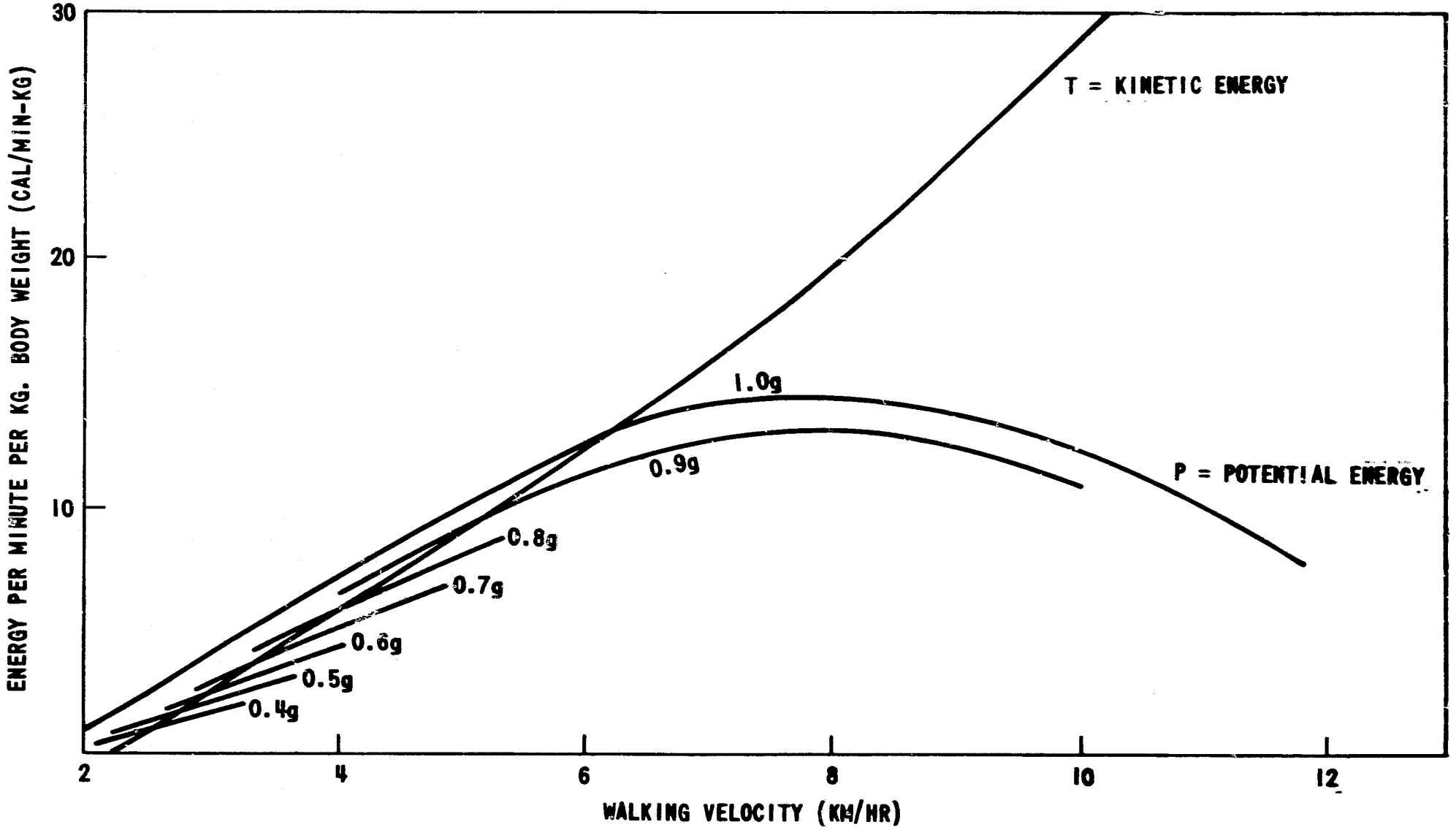

FIGURE 13 - MEASURED VERTICAL POTENTIAL AND HORIZONTAL KINETIC ENERGIES DURING WALKING. THE THIN LINE SHOWS OUR EXTRAPOLATION OF CAVAGNA'S P AND T CURVES (REF. 9)

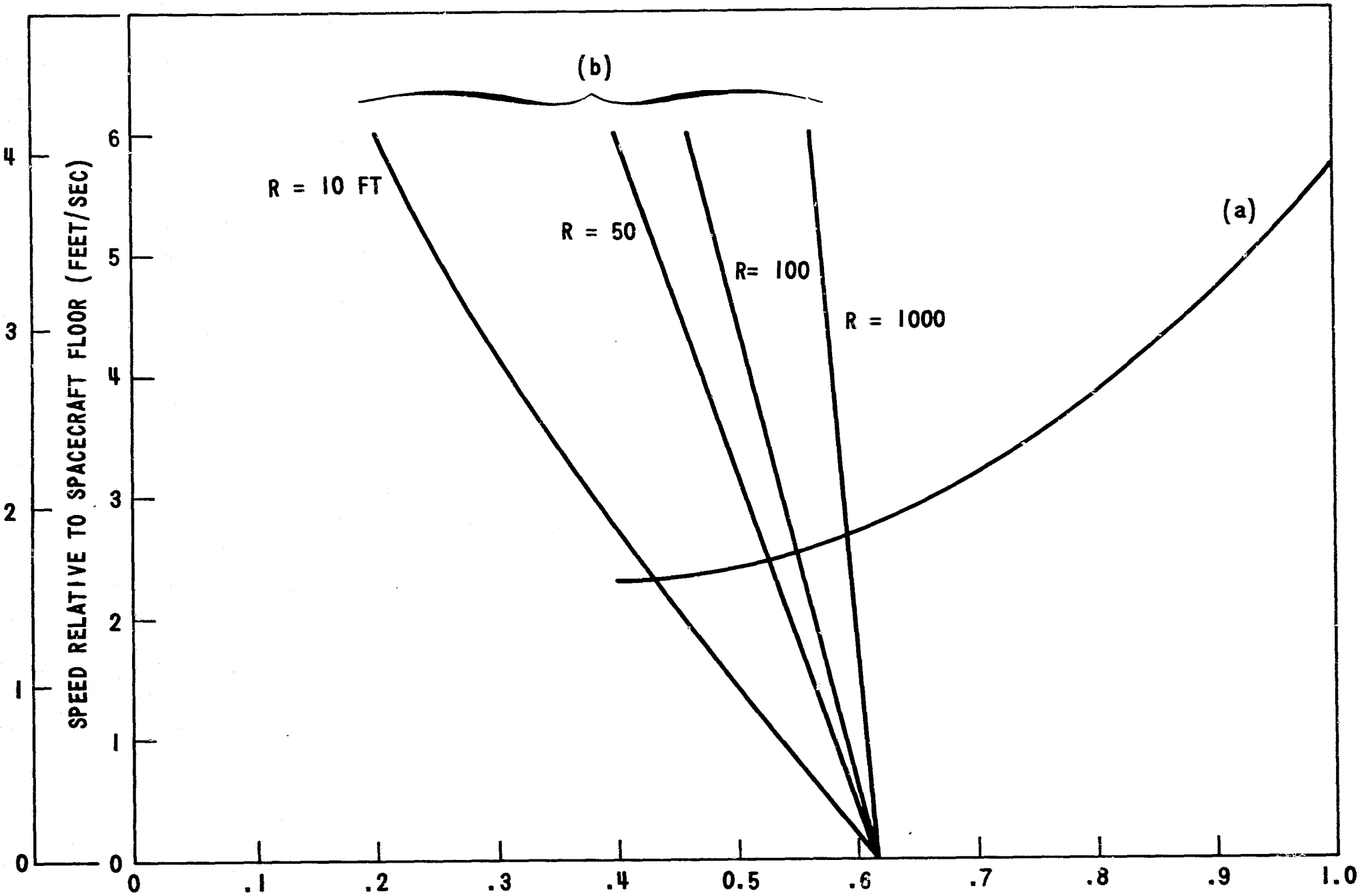

FIGURE 14 - (a) MAXIMUM WALKING VELOCITY (FROM FIGURE 13)
(b) "g LEVEL" AT FLOOR OF SEVERAL SPACECRAFT DESIGNS HAVING A NOMINAL LEVEL OF 0.617g

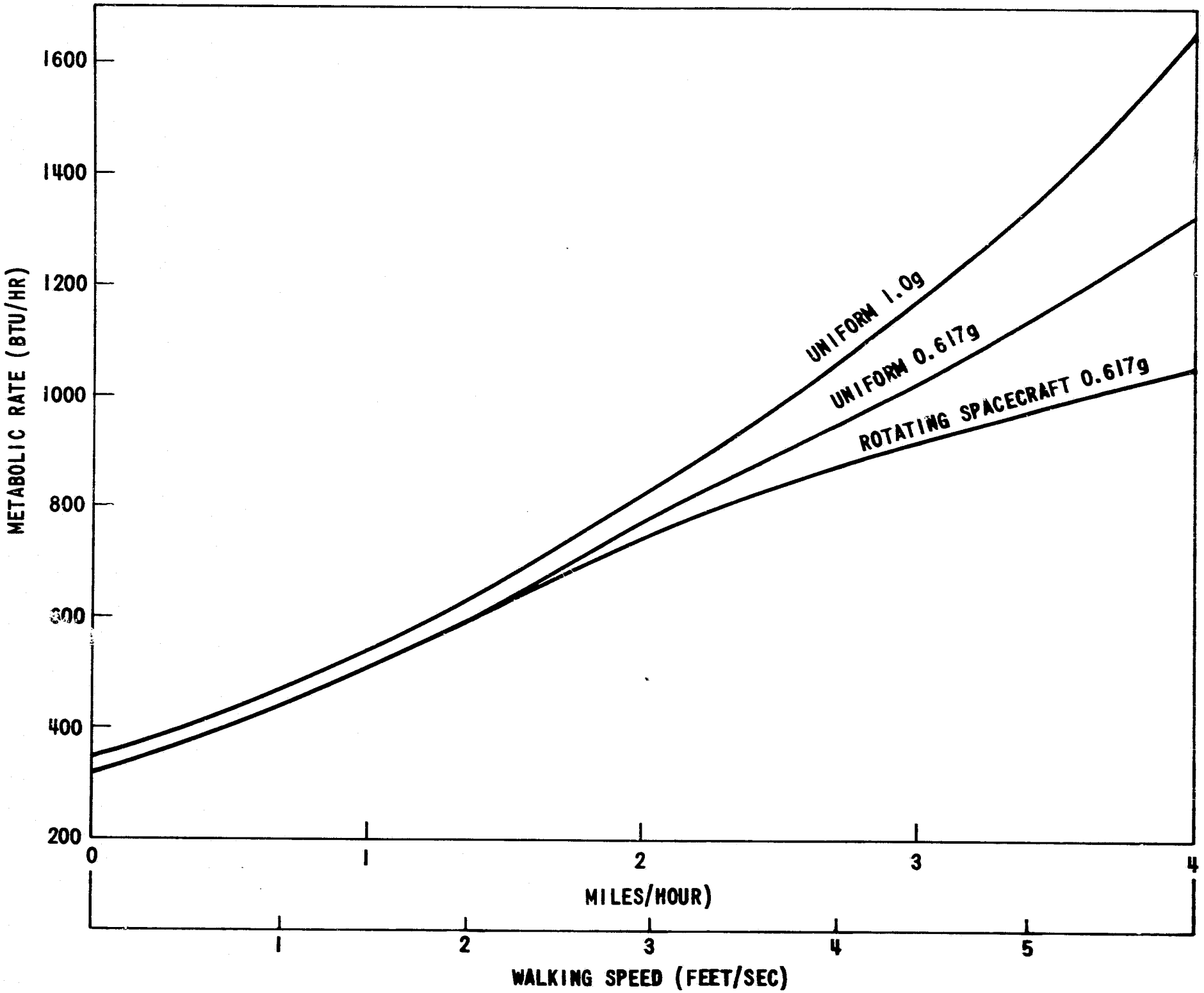

FIGURE 15 - TOTAL ENERGY EXPENITURE OF WALKING IN DIFFERENT ENVIRONMENT

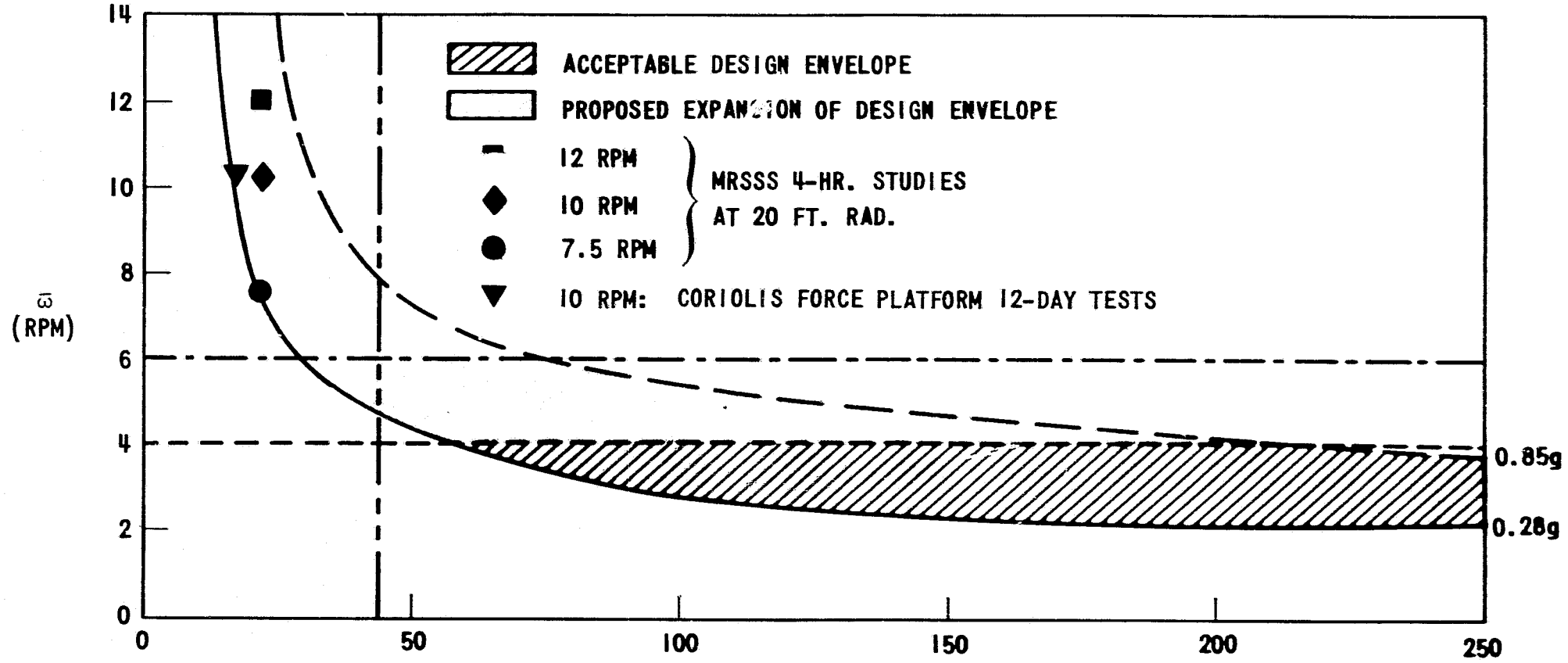

FIGURE 16 - BIOLOGICAL DESIGN LIMITS IN A ROTATING SPACE VEHICLE. (REF. 15)

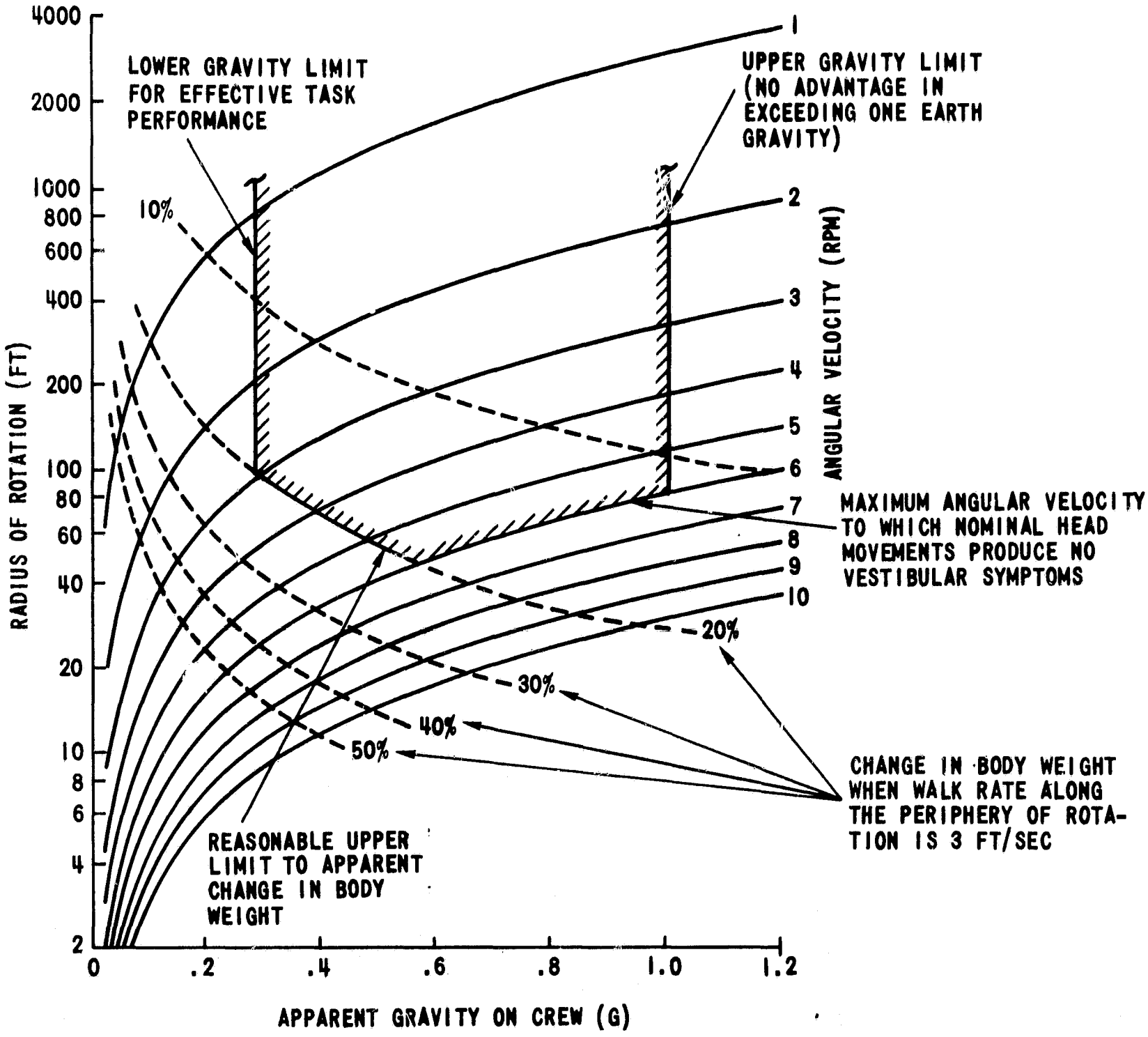

FIGURE 17 - PRELIMINARY TOLERABLE LIMITS FOR ACCEPTABLE HUMAN PERFORMANCE IN ROTATING SPACE SYSTEMS (FROM REF. 17)

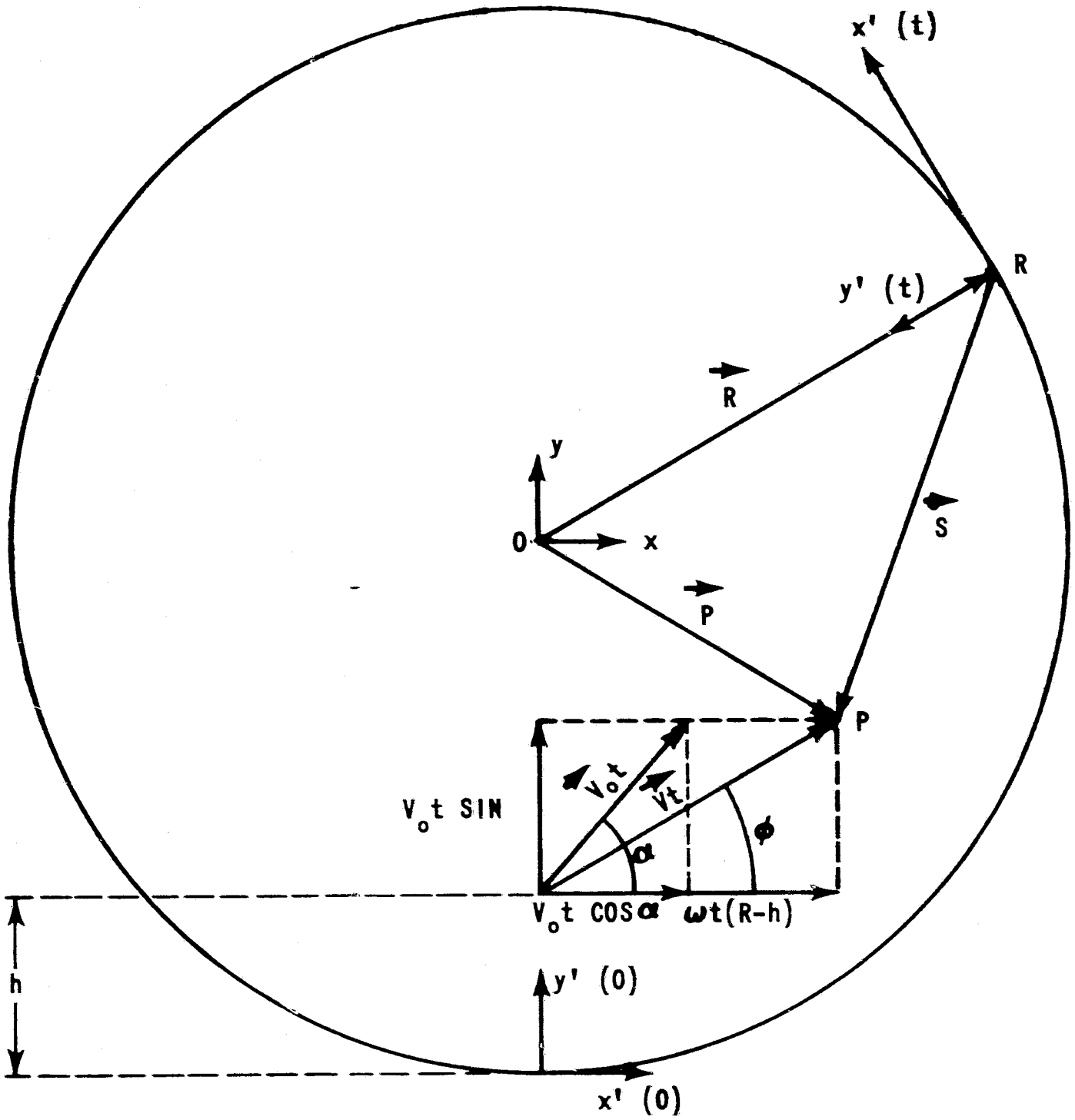

FIGURE 18 - PARTICLE AND RIM POSITIONS DURING FREE FALL
(INERTIAL FRAME)

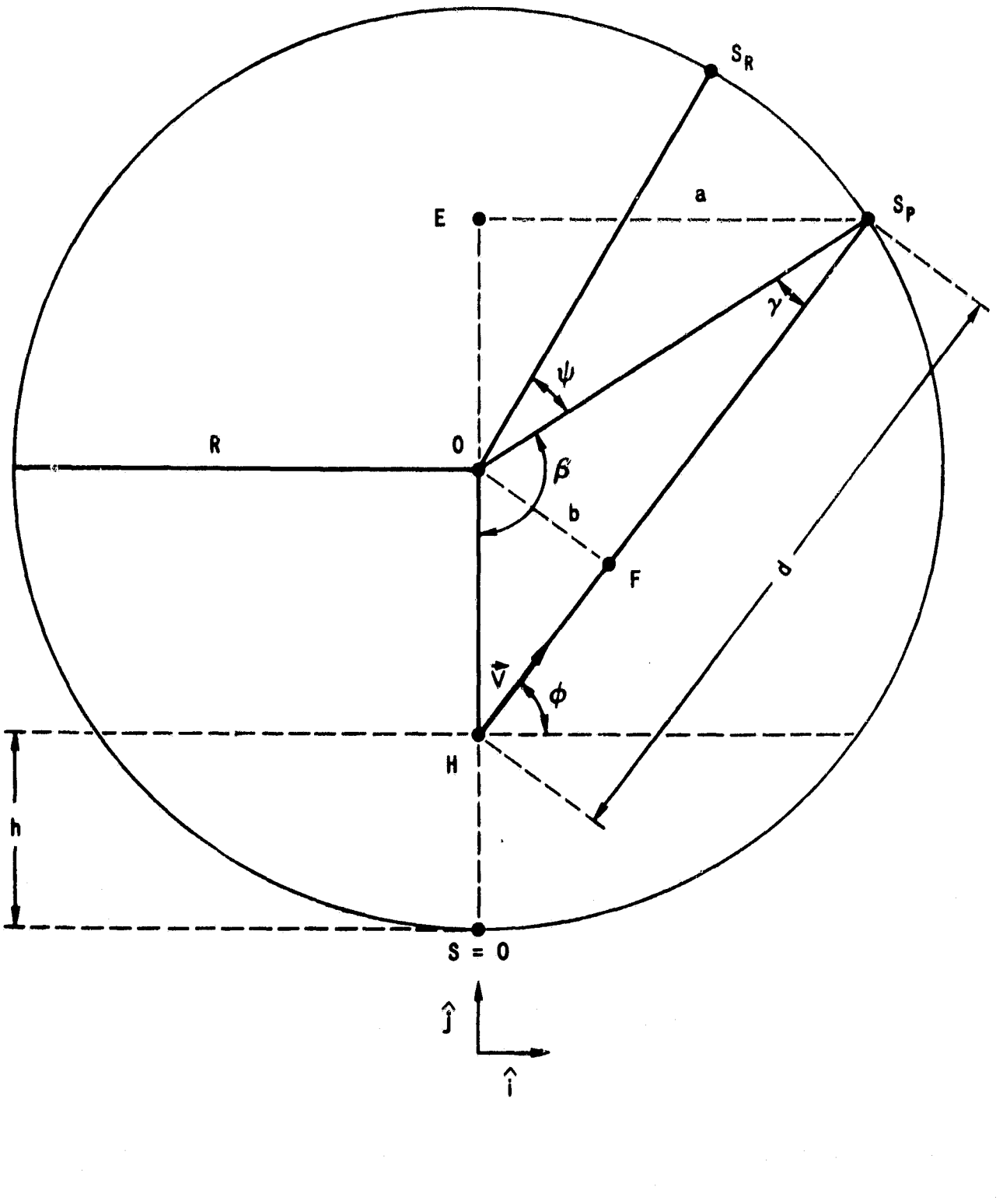

FIGURE 19 - PARTICLE AND RIM POSITIONS AT TIME OF IMPACT (INERTIAL FRAME)

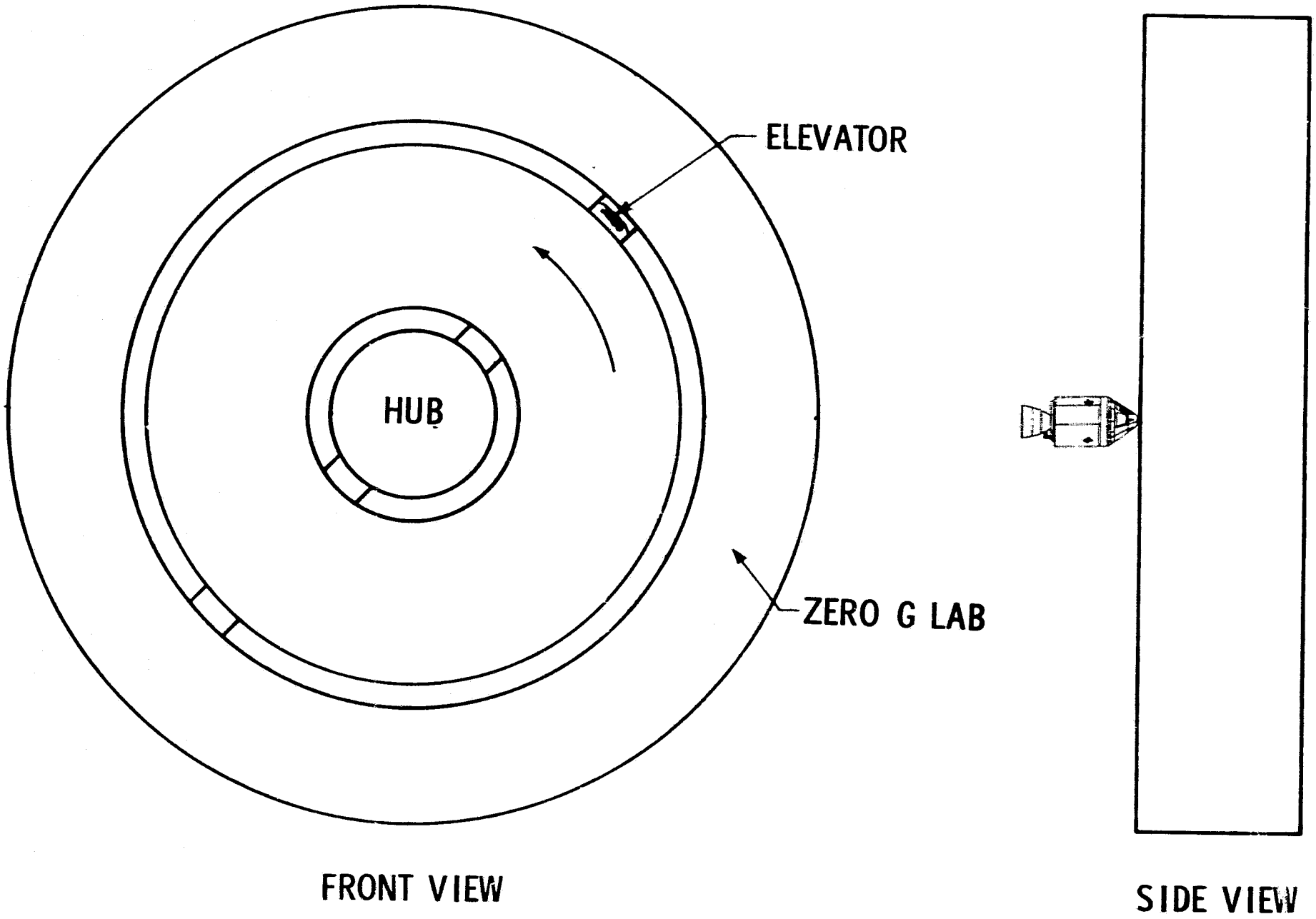

FIGURE 20 - A SIMPLE ANNULAR SPACE STATION CONFIGURATION

APPENDIX A

DERIVATION OF TRAJECTORY AND VELOCITY EQUATIONS FOR FREE FALL CONDITIONS

The system is a cylinder of radius R rotating about its axis with a constant angular velocity ω (Figure 1). A particle is released at time zero ($y = -(R-h)$, $x = 0$) from a height h above the rim with an initial velocity v_o at an angle α, where v_o and α are measured with respect to the rotating frame, (x', y'). The x,y coordinates define an inertial frame.

Viewed from an inertial frame centered at the axis of rotation, the particle always travels in a straight line until it intercepts the rim, and the rim travels along the arc of a circle of radius R. In this system at an arbitrary time, t, the particle has coordinates (Figure 18):

$$P_x = \omega(R-h)t + v_o t \cos \alpha$$

$$P_y = -(R-h) + v_o t \sin \alpha$$

The first term in the P_x equation represents the motion imparted by the rotating system, and the second term comes from the velocity, v_o, relative to the rotating system. In the y direction, the only motion is due to the vertical component of v_o; the first term is the zero-time y position.

A point fixed on the rim is described by:

$$R_x = R \sin \omega t$$

$$R_y = -R \cos \omega t$$

Therefore, the distance between the particle and rim is (see Figure 18):

$$\vec{S} = \vec{P} - \vec{R}$$

or, in components,

$$S_x = P_x - R_x$$

$$S_x = (R-h)\,\omega t + v_o t \cos \alpha - R \sin \omega t \qquad \text{(A-1)}$$

$$S_y = P_y - R_y$$

$$S_y = -(R-h) + v_o t \sin \alpha + R \cos \omega t \qquad \text{(A-2)}$$

This is the description of the particle-to-rim distance as viewed from the inertial frame. To describe the motion viewed from the rotating frame of reference, we must rotate the coordinate system by angle $\theta = \omega t$. Using primed symbols for the particle's position in a frame fixed at R on the rim, we have:

$$\vec{S}' = \begin{pmatrix} \cos \omega t & \sin \omega t \\ -\sin \omega t & \cos \omega t \end{pmatrix} \vec{S}$$

or,

(A-3) $$S_x' = S_x \cos \omega t + S_y \sin \omega t$$

(A-4) $$S_y' = -S_x \sin \omega t + S_y \cos \omega t$$

Substituting (A-1) and (A-2) into (A-3) and (A-4) gives:

(A-5) $$S_x' = (R-h)(\omega t \cos \omega t - \sin \omega t) + v_o t \cos(\omega t - \alpha) \equiv x'$$

(A-6) $$S_y' = R - (R-h)(\omega t \sin \omega t + \cos \omega t) - v_o t \sin(\omega t - \alpha) \equiv y'$$

Equations (A-5) and (A-6) are the expressions for the position of the particle, at any arbitrary time, t, relative to the point on the rim below which the particle was released at time zero as viewed in the reference frame of the rotating system.

To find the particle's velocity $\vec{U}$, relative to the rim, we calculate the time derivative of equations (A-5) and (A-6):

(A-7) $$U_x = \frac{d}{dt}(x')$$

$$= -(R-h)\omega^2 t \sin \omega t + v_o \cos(\omega t - \alpha) - v_o \omega t \sin(\omega t - \alpha)$$

(A-8) $$U_y = \frac{d}{dt}(y')$$

$$= -(R-h)\omega^2 t \cos \omega t - v_o \sin(\omega t - \alpha) - v_o \omega t \cos(\omega t - \alpha)$$

This completes the derivation of the equations describing the velocity and trajectory of particles in free fall as seen in the rotating frame of reference.

APPENDIX B

TIME OF FLIGHT AND POINT OF IMPACT OF PARTICLES IN FREE FALL WITH ARBITRARY INITIAL VELOCITY AND POSITION

A cylinder of radius R rotates about its axis with angular velocity ω. We want to calculate the time required for the particle to impact with the wall at radius R after its release inside the spacecraft. In the inertial frame (Figure 19), the particle begins free flight starting at a height h above the floor. It has a constant velocity $\vec{V}$ at an angle ϕ measured from a direction perpendicular to the radius at time zero. It continues in this direction in a straight line until it intercepts the floor at S_p in Figure 19. Let d be the distance traveled before it hits. The time of flight for the particle is:

$$T = \frac{d}{|\vec{V}|} \tag{B-1}$$

and the arc distance around the rim from the point below which the particle was released to the point of impact is

$$S_p = R\beta \text{ from Figure 19.} \tag{B-2}$$

During the time of particle transit, the rim has traveled an arc distance

$$S_R = R\omega T \tag{B-3}$$

Therefore, the apparent point of impact (angular distance traveled) as seen by an observer on the floor is

$$\psi = \frac{1}{R}(S_R - S_p)$$

$$= \omega T - \beta \text{ from (B-2) and (B-3).} \tag{B-4}$$

Next, we derive the quantities needed to calculate T and ψ in terms of the initial velocity and position as seen by an observer fixed in the cylinder and rotating with it. These are the quantities which are "real" and measurable to him.

When the particle is released, its velocity, $\vec{V}$, in the inertial frame is the vector sum of the velocity imparted by the rotating frame, $\omega(R-h)\hat{i}$ plus its velocity relative to the rotating frame $\vec{V}_o = (|\vec{V}_o|\cos\alpha)\hat{i} + (|\vec{V}_o|\sin\alpha)\hat{j}$. Here, $\hat{j}$ is the unit vector parallel to the radius through the particle at time zero, $\hat{i}$ is perpendicular to $\hat{j}$, and α is the angle with which it leaves, as seen in the rotating frame. Therefore (see Figure 19), we have (letting $v_o = |\vec{V}_o|$):

$$\vec{V} = [\omega(R-h) + v_o \cos\alpha]\hat{i} + (v_o \sin\alpha)\hat{j} \tag{B-5}$$

$$\tan\phi = \frac{v_o \sin\alpha}{\omega(R-h) + v_o \cos\alpha} \tag{B-6}$$

$$|\vec{V}| = [(\omega(R-h) + v_o \cos\alpha)^2 + (v_o \sin\alpha)^2]^{1/2} \tag{B-7}$$

The inertial distance of the flight, d, is related to the length a in the right triangles ES_pH and ES_pO (Figure 19) by

$$a = d \sin(\tfrac{\pi}{2} - \phi) = R \sin(\pi - \beta) \tag{B-8}$$

The length b in right triangles OFS_p and OFH is

$$b = R \sin\gamma = (R-h) \sin(\tfrac{\pi}{2} - \phi) \tag{B-9}$$

and the sum of angles in the triangle OHS_p is

$$\pi = \beta + \gamma + \tfrac{\pi}{2} - \phi \tag{B-10}$$

From these relationships:

$$d = \frac{\sin\beta}{\cos\phi} \text{ from (B-8)} \tag{B-11}$$

$$\beta = \tfrac{\pi}{2} + \phi - \gamma \text{ from (B-10) (see also below)} \tag{B-12}$$

$$\gamma = \sin^{-1}[(1 - \tfrac{h}{R})\cos\phi] \text{ from (B-9)} \tag{B-13}$$

Substituting (B-13) and (B-12) into (B-11) gives:

$$d = \frac{R \sin\{\tfrac{\pi}{2} + \phi - \sin^{-1}[(1 - \tfrac{h}{R})\cos\phi]\}}{\cos\phi} \quad 0 \le \phi \le \frac{3\pi}{2} \tag{B-14a}$$

It can be shown that (B-14a) is valid for all ϕ in the range $0 \le \phi \le \frac{3\pi}{2}$, but that when $\frac{3\pi}{2} \le \phi \le 2\pi$, equation (B-12) for β is altered (because β and ϕ are measured from different zero directions). This yields:

$$(B\text{-}14b) \quad d = \frac{R \sin\{-\frac{3\pi}{2} + \phi - \sin^{-1}[(1 - \frac{h}{R})\cos\phi]\}}{\cos\phi} \quad \frac{3\pi}{2} \leq \phi \leq 2\pi$$

Therefore, the time of flight can be calculated from (B-1), using (B-6) and (B-14a or b) for d and (B-7) for $|\vec{V}|$. The angular displacement ψ, measured from the starting place to the point of impact in the rotating frame, can be calculated from (B-4), using (B-1) for T and (B-12), (B-13), and (B-6) for β.

In summary, the time of flight, T, is

$$(B\text{-}15) \quad T = \frac{R \sin\beta}{|\vec{V}|\cos\phi}$$

$$(B\text{-}6) \quad \text{where } \tan\phi = \frac{v_o \sin\alpha}{v_o \cos\alpha + \omega(R-h)}$$

$$(B\text{-}7) \quad |\vec{V}| = [(\omega(R-h) + v_o \cos\alpha)^2 + (v_o \sin\alpha)^2]^{1/2}$$

$$(B\text{-}16) \quad \text{and} \quad \beta = \frac{\pi}{2} + \phi - \sin^{-1}[(1 - \frac{h}{R})\cos\phi] \text{ if } 0 \leq \phi \leq \frac{3\pi}{2}$$

$$(B\text{-}17) \quad \beta = -\frac{3\pi}{2} + \phi - \sin^{-1}[(1 - \frac{h}{R})\cos\phi] \text{ if } \frac{3\pi}{2} \leq \phi \leq 2\pi$$

The angular distance from the origin to the landing point is:

$$(B\text{-}4) \quad \psi = \omega T - \beta$$

These equations enable us to calculate T and ψ from the initial velocity v_o and α.

If $v_o = 0$, then $\phi = 0$ and the expressions for T and ψ simplify to

$$(B\text{-}18) \quad T = \frac{R \sin[\frac{\pi}{2} - \sin^{-1}(1 - \frac{h}{R})]}{\omega(R-h)}$$

$$= \frac{R[2\frac{h}{R} - (\frac{h}{R})^2]^{1/2}}{\omega(R-h)}$$

$$(B\text{-}19) \quad = \frac{[2\frac{h}{R} - (\frac{h}{R})^2]^{1/2}}{\omega(1-\frac{h}{R})}$$

$$\psi = \omega T - \frac{\pi}{2} + \sin^{-1}(1 - \frac{h}{R})$$

$$(B\text{-}20) \quad = \frac{[2\frac{h}{R} - (\frac{h}{R})^2]^{1/2}}{(1-\frac{h}{R})} - \cos^{-1}(1 - \frac{h}{R})$$

To show that ψ, as defined by B-20 (i.e. for $v_o = 0$) is always positive, note that ψ can be expressed in terms of an auxiliary angle δ, as follows:

(B-21) $$\psi = \tan \delta - \delta$$

This is always positive, by definition of the tangent function. The positive nature of ψ can also be seen from eq. A-7 for the x-compnent of the velocity.

Therefore the particle always drifts behind the observer as it falls.

APPENDIX C

THE ERROR IN POUNDING A NAIL WHILE HAMMERING IN A ROTATING ENVIRONMENT

In this appendix the horizontal deviation of the impact point of a vertically driven hammer of mass m is calculated. The hammer is driven by a constant vertical force F toward a target on the space station floor located a distance h below the starting point. We derive the appropriate trajectory equation and calculate the deviation using a numerical iteration procedure.

As seen in the reference frame of the rotating system, the acceleration of the hammer is:

$$\vec{A} = [\omega^2(R-h) + \frac{F}{m}]\hat{j} - 2\vec{\omega} \times \vec{V} - \vec{\omega}\times(\vec{\omega} \times \vec{r}) \tag{C-1}$$

where $\hat{j}$ is a unit vector in the vertical direction, $\vec{V}$ is the velocity of the hammer, and $\vec{r}(t)$ is the vector position of the hammer relative to its starting point. Since the hammer is driven vertically down, r will be predominately in the $\hat{j}$ direction. Then $-\vec{\omega}\times(\vec{\omega} \times \vec{r})$ is $\omega^2 r\hat{j}$ and can be incorporated into the first term of $\vec{A}$.

$$\vec{A} = [\omega^2(R-h + r(t)) + \frac{F}{m}]\hat{j} - 2\vec{\omega} \times \vec{V}(t) \tag{C-2}$$

To obtain a formula for the coordinates, $\vec{r}(t)$, we integrate (C-2) twice over time:

$$\vec{V} = \int_o^t \vec{A}\, dt$$

$$= [(\omega^2(R-h + r) + \frac{F}{m})\int_o^t dt]\hat{j} - 2\vec{\omega} \times \int_o^t \vec{V}\, dt$$

$$= (kt)\hat{j} - 2\vec{\omega} \times \vec{r} \tag{C-3}$$

Although $\vec{r}(t)$ is a function of time, it is assumed to change very little relative to R-h during the motion and can thus be considered constant over the time interval of integration in the first term above.

A second integration yields $\vec{r}(t)$:

$$\vec{r}(t) = \int_o^t \vec{V}(t)dt$$

$$= (1/2\ kt^2)\hat{j} - 2\vec{\omega} \times \int_o^t \vec{r}(t)dt \qquad (C-4)$$

Since $\vec{\omega}$ is a vector in the z-direction, the cross product can be written:

$$\vec{\omega} \times \vec{r}(t) = (-\omega r_y)\hat{i} + (\omega r_x)\hat{j}$$

where r_x and r_y are the components of $\vec{r}$ in the $\hat{i}$ and $\hat{j}$ directions. Therefore, $\vec{r}$ can be written:

$$\vec{r}(t) = (1/2\ kt^2)\hat{j} - (2\omega \int_o^t r_x(t)dt)\hat{j} + (2\omega \int_o^t r_y(t)dt)\hat{i} \qquad (C-5)$$

This equation for $\vec{r}$ can be evaluated by an iteration procedure where the initial approximation, $\vec{r}_o$, neglects the Coriolis terms.

$$\vec{r}_o(t) = (1/2\ kt^2)\hat{j}$$

Successive approximations are calculated from (C-5) using the previous approximations as follows:

$$\vec{r}_m(t) = (1/2\ kt^2)\hat{j} - (2\omega \int_o^t r_{m-1,x}(t)dt)\hat{j} \qquad (C-6)$$

$$+ (2\omega \int_o^t r_{m-1,y}(t)dt)\hat{i}$$

At each stage of the iteration we evaluate an approximation for the time of hit T_m by calculating the time at which the y component of r_m (in the $\hat{j}$ direction) is equal to the height h abcve the target where the hammer starts. With this value of T_m, the horizontal component, $r_{m,x}$ can be found.

The first few evaluations of $\ddot{r}$ are given in the following table:

m	$(r_{m,y})$	$(r_{m,x})$
0	$1/2\ kt^2$	0
1	$1/2\ kt^2$	$\frac{2\omega k}{2\times 3}\ t^3$
2	$1/2\ kt^2 - \frac{(2\omega)^2 k}{2\times 3\times 4}\ t^4$	$\frac{2\omega k}{2\times 3}\ t^3$
3	$1/2\ kt^2 - \frac{(2\omega)^2 k}{2\times 3\times 4}\ t^4$	$\frac{2\omega k}{2\times 3} t^3 - \frac{(2\omega)^3 k}{2\times 3\times 4\times 5}\ t^5$

This procedure is repeated until $(R_m)\hat{i}$ converges to some stable value.

As an example, a hammer weighing 5 lb. on earth is driven downward with a force of 10 lb. starting at a height h = 1.0 foot above the target in a rotating space station of radius 50 feet and ω = 6 rpm ($\pi/5$ rad/sec). Then in equation (C-3) $k = \frac{10}{5}\ (32.1720) \times (\frac{\pi}{5})^2 (50 - 1 + 1) = 84.0233$ and our numerical values are:

m	T_m(seconds)$_{(5\ lb.)}$	$r_{m,x}$(inches)
0	0.1542	0.0000
1	0.1542	0.7680
2	.1545	0.7788
3	.1545	.7671

Therefore, the hammer would miss the mark by approximately 3/4 of an inch.